KTH Byggvetenskap

Measurement and Evaluation of Cable Forces in the Älvsborg Bridge

Alice Eklund

Structural Design and Bridges
Royal Institute of Technology
Stockholm, 2006

TRITA-BKN, Master thesis 235

Measurement and Evaluation of Cable Forces in the Älvsborg Bridge

Supervisor:	Doc. Stud. Andreas Andersson (KTH)
Co-supervisor:	Dr. Raid Karoumi (KTH)
Examiner:	Prof. Håkan Sundquist (KTH)
Other advisers:	Doc Stud. Richard Malm (KTH)
	Lab.Engineer Stefan Trillkott (KTH)
	Lab.Engineer Claes Kullberg (KTH)

ABSTRACT

In this thesis the dynamic behaviour of the Älvsborg Bridge has been monitored. The bridge is situated in Gothenburg and was built in the 1960th. By measuring the responses to vibration of the cables and mid span of the bridge, parameters are obtained that can be used for verification of a finite element model made by the Danish company Ramböll. Their model is built up in order to classify the Älvsborg Bridge at the request of the Swedish National Road Administration (Vägverket).

The measurements were carried out in November 2005 coordinated by the Royal Institute of Technology (KTH).

The frequency peaks from the mid span measurements are presented in the table below and are possible global frequencies of the bridge.

Mode number:		1	2	3	4
Hanger 6	Horizontal:	0,19	0,45	0,65	0,76
	Vertical:	0,22	0,39	0,50	0,76
Middle of bridge:	Horizontal:	0,51	0,65	1,01	
	Vertical:	0,29	0,39	0,51	0,77

Table i *The peaks in the frequency spectra for horizontal and vertical vibrations of the bridge in the mid span have been picked out. Measurements were done by hanger 6 and in the middle of the span. The unit is Hz.*

The axial forces in the four side span cables are determined to 69 MN in the northern cables and 71 MN in the southern cables.

In one splay chamber all the strands from one side span cable has been analysed in order to compare the sum of the axial forces in the 85 strands with the axial force in the main cable. Calculations based on measured responses show that the mean axial force of one strand is 852 kN which gives a total force of 72.4 MN.

SAMMANFATTNING

Älvsborgsbron i Göteborg håller på att klassningsberäknas av Ramböll i Danmark på uppdrag av Vägverket. Det görs för att veta vilken typ av trafik som kan passera över bron med avseende på brons hållfasthet. Ramböll har byggt upp en datamodell med finit elementmetod som ska testas för olika belastningsfall. För att kunna lita på att modellen stämmer överens med verkligheten vill man kalibrera den mot uppmätta data från den riktiga bron.

I mitt examensarbete har jag, Alice Eklund, tillsammans med Andreas Andersson (doktorand på KTH), Stefan Trillkott (laboratoriechef KTH) och Cleas Kullberg (1: e forskningsingenjör KTH) utfört mätningar på Älvsborgsbron under en vecka i november 2005. De parametrar vi tittat på är egenfrekvenser för bron och dess kablar.

Andra personer på plats under denna vecka var två industriklättrare från Rope Access som hjälpte till med monteringen av mätutrustningen och Per Thunstedt från Vägverket som tog hand om avstängning av delar av bron när det var nödvändigt.

Figur i *Simon (från Rope Access) och Alice (rapportförfattaren) på en av bakstagskablarna.*

Huvudmålet med rapporten är att beskriva tillvägagångssätt vid mätningarna och presentera globala egenfrekvenser för bron och beräkna kabelkraften för samtliga fyra bakstag.

För ett utav bakstagen har även mätningar på alla 85 delkablarna gjorts för att jämföra summan av krafterna med totala kraften för huvudkabeln. Dessa mätningar gjordes inne i den nordöstra spridningskammaren.

Vibrationer har mätts med accelerometrar. De uppmätta accelerationerna har sedan omvandlats till frekvenser genom Fourier transformation. Ur vibrationsspektra har topparna för egenfrekvenserna plockats ut. Noggrannheten hos frekvenserna uppskattas till minst ±0.01 Hz.

Brons globala egenfrekvenser undersöktes i brons fjärdedelspunkt och i brobanans mitt.

	Mod nr:	1	2	3	4
Hängare 6	Horisontal:	0,19	0,45	0,65	0,76
	Vertikal:	0,22	0,39	0,50	0,76
Bromitt:	Horisontal:	0,51	0,65	1,01	
	Vertikal:	0,29	0,39	0,51	0,77

Tabell i *Älvsborgsbrons globala egenfrekvenser undersöks. Här presenteras synliga toppar i frekvensspektra i horisontell och vertikal riktning i fjärdedelspunkten och i bromitt.*

Krafterna i bakstagen beräknas utifrån förenklingen att skjuvdeformation saknas med följande formel:

$$S = \left(\frac{2 \cdot f_k \cdot l}{k}\right)^2 \cdot \frac{m}{\kappa^2}$$

S är axialkraften som beror av längden på kabeln *l*, massan per längdenhet *m*, modnummer *k*, egenfrekvensen f_k för egenmod k samt κ som har olika uttryck beroende av inspänningsgrad. Nedan visas uttrycken för κ_c och κ_s där c står för clamped (fast inspänd) och s står för simple supported (fritt upplagd). Här kommer även kablarnas böjstyvhet, *EI*, med i beräkningarna.

$$\kappa_c = 1 + \frac{2}{\beta} + \frac{1}{\beta^2} \cdot \left[4 + \frac{(k \cdot \pi)^2}{2}\right] \qquad \kappa_s = \sqrt{1 + \left(\frac{k \cdot \pi}{\beta}\right)^2} \qquad \beta = l \cdot \sqrt{\frac{S}{EI}}$$

Resultaten för kablarnas axiella krafter är framräknade till 69 MN för de norra bakstagen och 71 MN för de södra.

Summan av krafterna i spridningskammaren beräknades till 72.4 MN.

TABLE OF CONTENTS

1 Introduction

Figure 1:1 *The Älvsborg Bridge. View from south west, Sundqvist (2005).*

1.1 Background

The Älvsborgs Bridge was taken into use in November 1966 (Asplund (1966)). At this time the prescribed standards for bridges in Sweden were different from today. It has been in the interest of *Vägverket*, the Swedish Road Administration and *Banverket*, the Swedish Railway Administration to reclassify the bridges in Sweden according to the present standards. To classify a bridge means that the bridge is analysed for its bearing capacity in terms of the traffic the bridge can carry. The results from the classification are maximum axle and bogie loads of the vehicles. On top of that an extra investigation on the bearing of military vehicles is carried out (http://www.vv.se).

The classification of the Älvsborg Bridge is accomplished by the Danish company *Ramböll* during the years 2005-2006. They are evaluating the bridge by creating a three dimensional finite element model of the bridge.

For verification of the calculated results *KTH,* the Royal Institute of Technology in Stockholm, have executed non-destructive testing on the Älvsborg Bridge during the year 2005. Before *KTH* was initiated in the project the Danish company *COWI konsult* had executed vibration measurements of the cables in the mid span of the bridge and all the hangers. Whereas the measurements executed by *KTH* that are presented in my thesis have a focus on the global vibrations of the bridge and the four stay cables. During 2005 the geometry of the main cable was measured by *Gatubolaget*. These measurements were repeated in 2006 since there were some doubts about the accuracy.

1.2 Aims and scope of the Study

The aims of this study are:

- Evaluate the axial force in the side span cables of the Älvsborg Bridge.
- Evaluate the sum of the axial forces of the strands in one of the four splay chambers.
- Present the global frequencies of the bridge.
- Present the measuring procedure in detail.

1.3 Structure of the Thesis

In Chapter 1, I wish to introduce the structure of the Älvsborg Bridge and the idea of today's evaluations and reclassification of the bridge. The properties of the cables that will be used further on in the report are presented.

The theoretical background is introduced in the following two chapters. Since the focus in the thesis is on the cables of the Älvsborg Bridge Chapter 2 introduces the dynamics of a cable. An analytical and a numerical way to calculate the axial force in the cables are described.

Chapter 3 deals with the theory of signal analysis.

The results in this thesis are received through non-destructive measurements using acceleration sensors placed at different parts of the structure when the structure is set in motion. This vibration testing is presented in detail in Chapter 4. The documentation of instrumentation and measuring procedure is one of the objectives in this report, and are intended to be clear and descriptive.

Signal analysis and the theories of dynamics are used to evaluate the data from the measurements in Chapter 5 where the results are presented. Chapter 6 concludes and some comparisons with the results from Ramböll are viewed.

For force evaluation an analytical expression is used that is hard to solve for other end conditions than simple supported or totally clamped. Therefore, a MATLAB code for calculations with other end conditions using the central difference method was executed and is attached in APPENDIX B1.

1.4 The Älvsborg Bridge

The Älvsborg Bridge was constructed between 1963 and 1966 in Gothenburg, Sweden. It was to be the largest suspension bridge in Scandinavia at that time (Samuelsson (1966:4)) and it had the longest span of all bridges in Sweden until 1997. Before the Älvsborg Bridge was built the only traffic pass over Göta Älv with high capacity was the Götaälv Bridge (*Götaälvbron*). Due to a growing city and traffic expansion the Älvsborg Bridge was constructed at the west end of the city and a few years later the Tingstad tunnel (*Tingstadstunneln*) was open for traffic at the eastern end of the river.

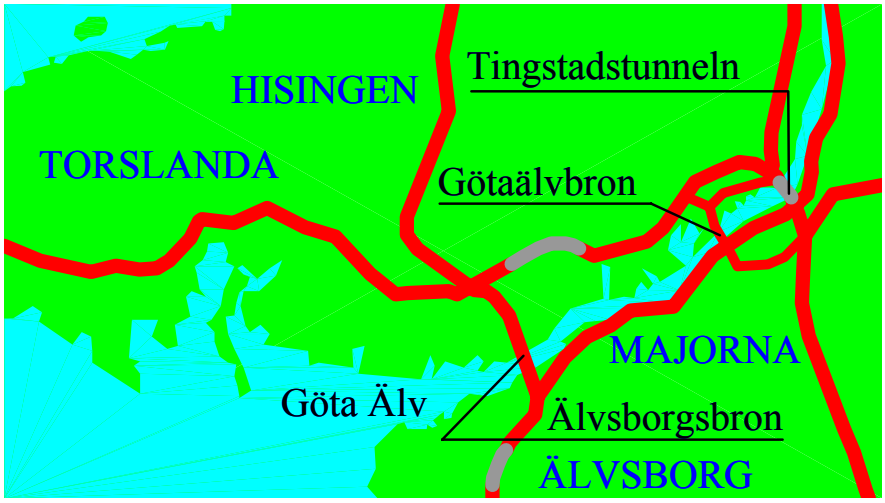

Figure 1:2 *Map of Gothenburg showing where the bridge is situated*

1.4.1 Structure of the Bridge

The structural idea of suspension bridges is to let cables carry the load to the supports and by that allow a light and wide mid span. To overcome large areas is the distinguishing quality of suspension bridges. According to Gimsing (1983) the cable supported bridges are competitive when they are to overcome a span of 250 meters or more.

In Figure 1:3 the mode of load carriage at the Älvsborg Bridge is outlined. The cable system consists of hangers at each side of the stiffener girder held up by the main cable. The main cable is supported by pylons and anchored to the ground.

Stiffening girder. In this bridge a truss.

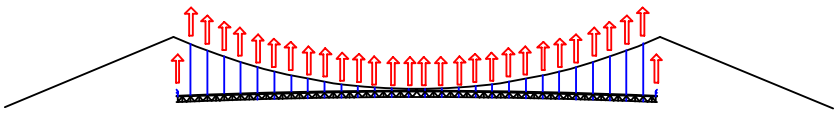

Cable system. The hangers are supporting the stiffening girder.

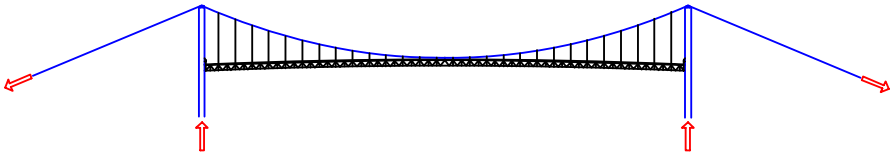

Pylons and main cables. The pylons are supporting the main cables.

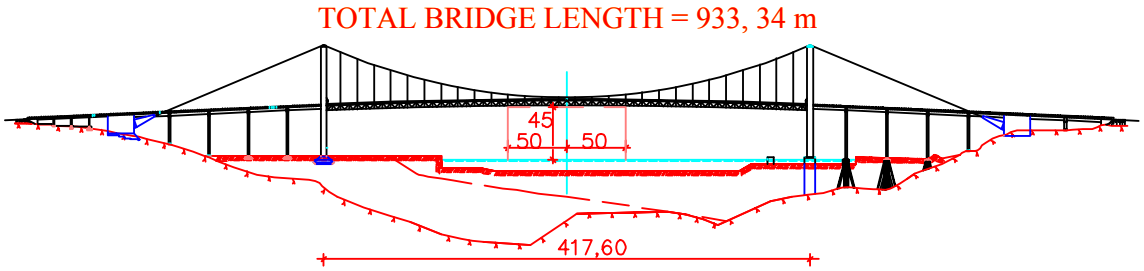

Figure 1:3 *Structure of the Älvsborg Bridge. Picture modified from AutoCAD drawing by Ramböll.*

The Älvsborg Bridge has a span of 417.6 meters between the pylons with a navigable passage width of 100 meters for a 45 meters vertical clearance, see Figure 1:3. The big span is motivated by the need for space due to ferry transports and also bad supporting foundation conditions that make it difficult to allow supports any closer to each other. The total bridge length is 933.3 meters. The width of the stiffener girder is 28.1 meters with two carriage-ways. Each carriage-way has three traffic lanes plus one bicycle lane on either side.

In Figure 1:4 the four major components of the structural system at the Älvsborg Bridge are pointed out (Gimsing (1983)).

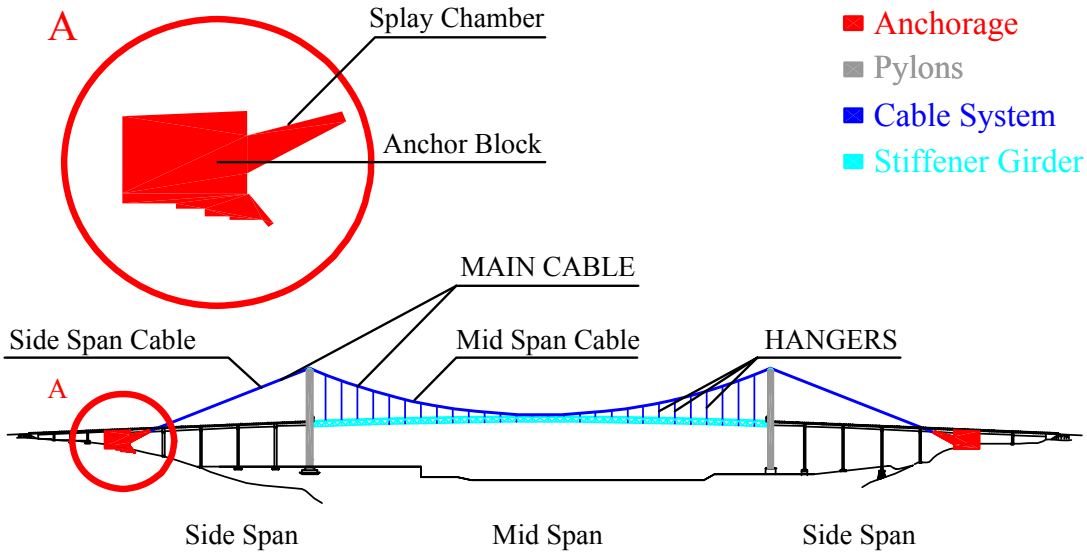

Figure 1:4 *Main structural components of a suspension bridge. Picture modified from AutoCAD drawing by Ramböll.*

The bridge deck in the side span is constructed of concrete whereas the bridge deck in the mid span, also called the stiffener girder, is a steel truss with a concrete carriage way.

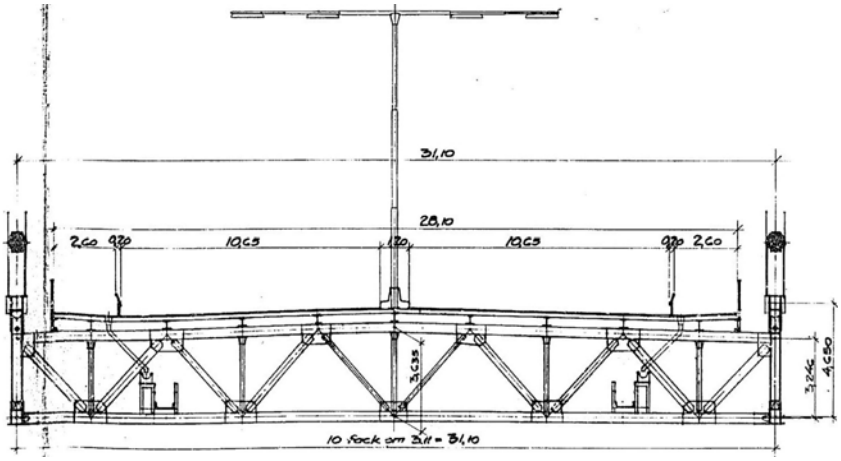

Figure 1:5 *Cross-section of the stiffener girder.*

The pylons are towers in shape of big concrete frames carrying up the main cable. The two columns of the frame have hollow rectangular cross-sections as well as the two transverse beams, see Figure 1:6. Inside the columns there are elevators for accessibility to the top of the pylons were the two saddles are guiding the main cables, see Figure 1:8. The height is about 95 meters off the ground.

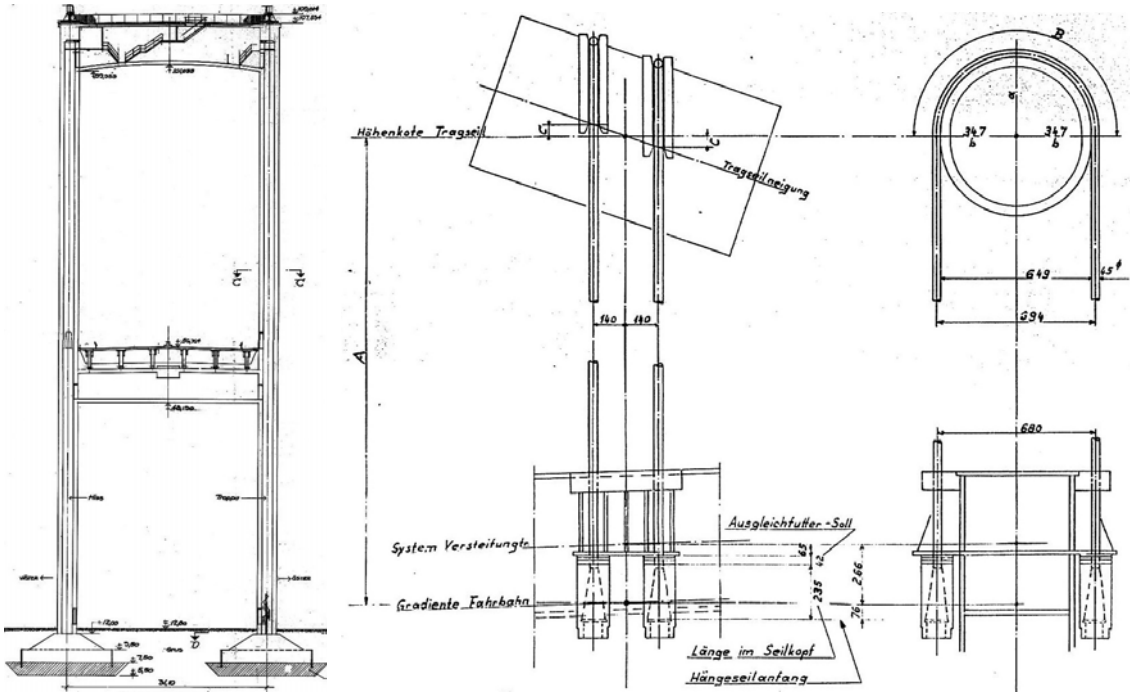

Figure 1:6 *One of the two frame-shaped pylons on the left drawing. The hanger on the right consists of two strands suspended from the main cable.*

The cable system can be divided into hangers and main cables. The hangers are connecting the stiffener girder to the main cable. At the Älvsborg Bridge the hangers consist of two strands suspended around the main cable, as in Figure 1:6. The hangers are distributed in mid span. Here the main cable is called the mid span cable. From the pylons the main cable is continuing down to the anchor blocks through the splay chamber. The anchor blocks are heavy weights of concrete that by gravity rest on the ground and keep the cables stressed. The side span cables between the pylon and the anchor could also be called the stay cables or the anchor cables. Their inclination is 42 %. When the cables enter the anchorage the strands of the cable are spread out in the splay chamber and clamped one and one into the anchor block wall (see Figure 1:11).

1.4.2 Properties of the Cable

In suspension bridge constructions the cables consist of thin wires of high performance steel (Gimsing (1983)). At the Älvsborg Bridge the wires are assembled in prefabricated strands as shown in Figure 1:7. 85 parallelly bundled strands with a diameter of 54.7 mm constitute the main cable.

There are different ways to organize the wires in the strand. The locked-coil strand used at the Älvsborg Bridge gives a smoother and tighter surface witch makes it corrosion-resistant and less sensitive to side pressures at the saddle and the anchorages. The wires in the locked-coil strands at the Älvsborg Bridge have different shapes. Round wires are parallel in the middle, surrounded by two layers of wedge shaped wires and one layer of Z-shaped helically winded wires. The strands are quite compact and should give a density of about 90 % compared to a solid cross-section with the same diameter according to Gimsing (1983). It is easier to bend them since they are twisted, each wire does not need to elongate or contract when the strand does. The negative aspect is that the twisted strand doesn't only get a lower bending stiffness but also looses strength. A typical value for the modulus of elasticity for this kind of strands is

E =170 GPa (Gimsing (1983)). The cables have bending stiffness due to the strand moment of inertia and the friction between the strands in the cable (Hewett-Packard CO (1994)).

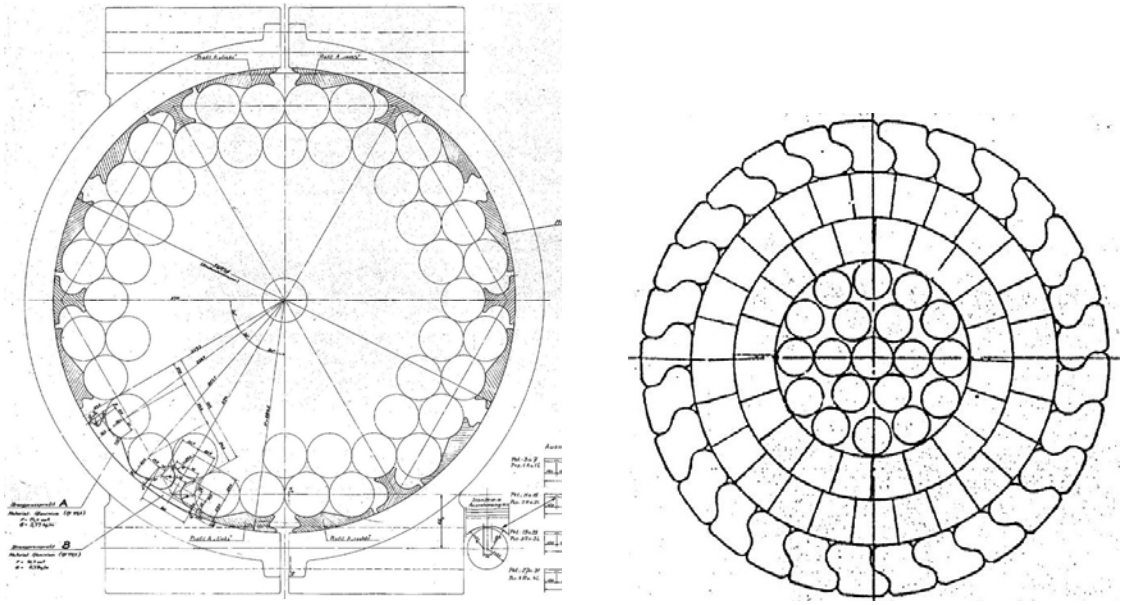

Figure 1:7 *A cross-section of the main cable is shown on the left. It consists of 85 parallel coiled-locked strands, pictured at the right.*

Strand:	Area:	2037 mm^2, ϕ54.7 mm	(Original drawing)
	Mass:	17.2 kg/m	(Original drawing)
	E-modulus, effective:	170 GPa	(Gimsing (1983))
	Ultimate load:	315 000 kg or 3.09 MN	(Original drawing)
	Effective load:	288 000 kg or 2.83 MN	(Original drawing)
Main cable:	Mass:	1534 kg/m	17.2·85 + 72 (Ramböll)
	E-modulus, effective:	163 GPa	
	Mean ultimate stress:	1.55 MPa	(Asplund (1966))

The supports of the main cable are pictured below:

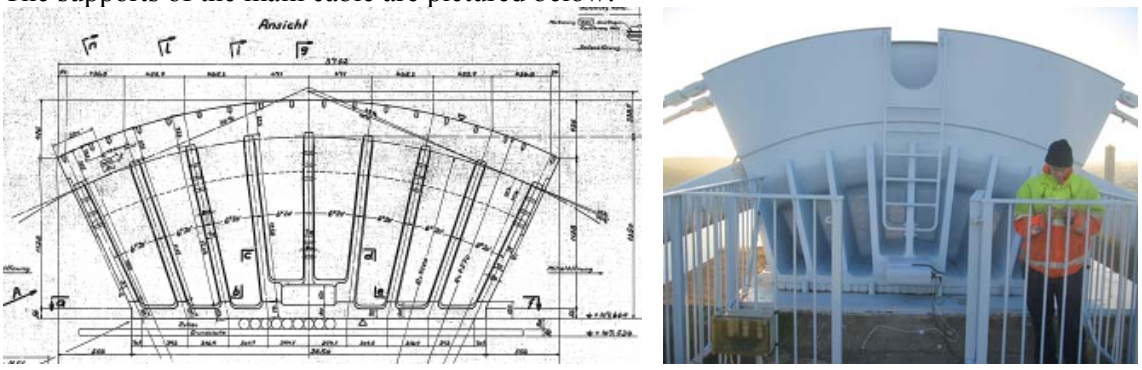

Figure 1:8 *Saddle supporting the cable on top of the pylon. The cable is fixed in its normal direction because of friction.*

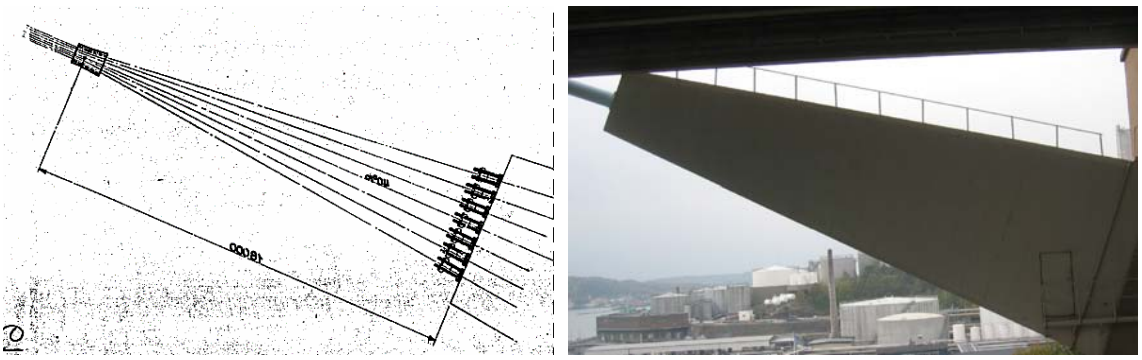

Figure 1:9 *The cable enters the splay chamber just below the bridge deck.*

Figure 1:10 *View from the inside of the splay chamber where the 85 strands are released from the cable coat.*

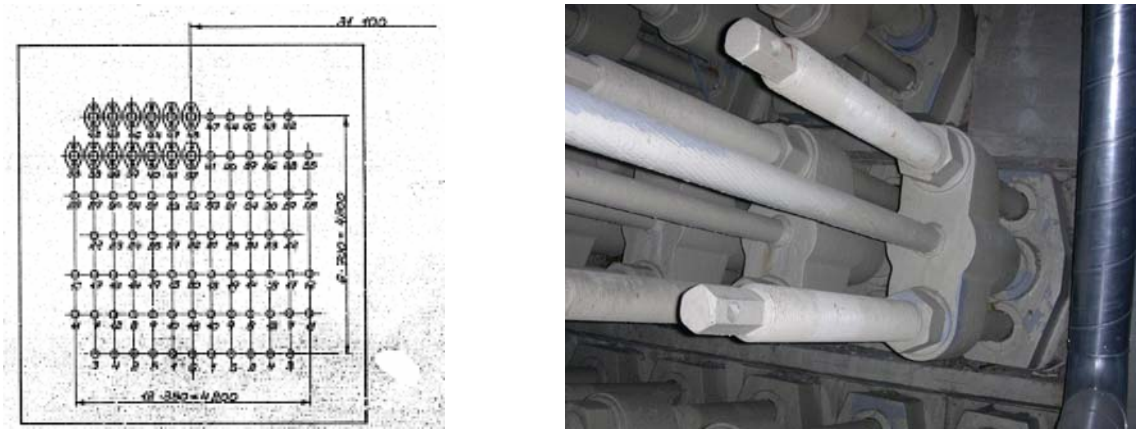

Figure 1:11 *The 85 strands are clamped into the back wall of the splay chamber.*

2 Dynamics of a Cable

Figure 2:1 *The main cable at the Älvsborg Bridge.*

2.1 Vibration Modes and Natural Frequencies

The concept of a string is used in theory for a cable or a wire without bending stiffness (*EI*). A string that is free to move between two points will move in a determined way when it is excited. In the same way as a string of an instrument emits the same tone each time it is set in motion as long as it is tensed in the same way. That means that a string with certain properties and axial force has pre-determined frequencies, or tones, that it will emit. These frequencies (f_{ks}) are called the natural frequencies. The excited string will move with more than one of its natural frequencies at the same time. Each natural frequency has a corresponding mode shape. The three first mode shapes of a taut string are shown in Figure 2:2.

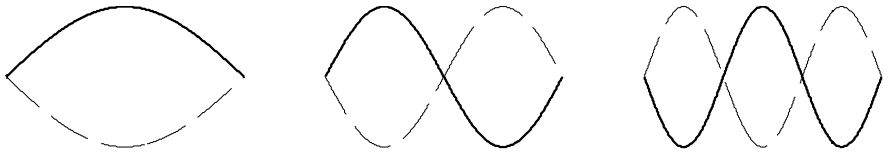

Figure 2:2 *The first three mode shapes for a taut string, starting at mode order one at the left.*

The natural frequency is the amount of periods the string performs in one second and can be derived from the equation below for a taut string (a string with an axial force), Geier (2004).

$$f_{ks} = \frac{k}{2 \cdot l} \cdot \sqrt{\frac{S}{m}} \qquad (2.1)$$

In the equation m stands for mass per unit length, S is the axial force in the string, l is the length and k is the mode order. From the formula some conclusion about the relationship between the properties of the string and the frequency can be made. Some of the conclusions are easy to understand from merely intuition:

- The more tensed the string is - the faster it vibrates
- The thinner and lighter the string is - the faster it vibrates
- The shorter the string is – the faster it vibrates
- The higher mode order - the faster it vibrates

Equation 2.1 is almost true for strings of an instrument since they are so slender that there bending stiffness almost equals zero. The thicker strings of a guitar are composed of several thin wires that are twisted to decrease the bending stiffness. The reason for the striving of eliminating the bending stiffness is to produce pure tones and corresponding overtones.

2.2 Describing a Cable

2.2.1 Analytically

A cable can be described by using the Euler-Bernoulli beam theory. This is a good approximation for slim beams and cables when the shear deformations and effect of rotary inertia are small Weaver, Timoshenko & Young (1990). This theory assumes that the cross-section stays normal to the middle line. For large cross-sections compared to the length of the beam the Timoshenko beam theory is more accurate.

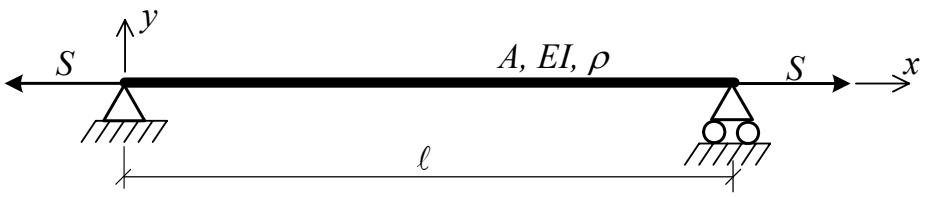

Figure 2:3 *Visualizing the parameters of a beam, Sundqvist.*

$$EI\cdot\frac{d^4}{dx^4}v(x,t) - S\cdot\frac{d^2}{dx^2}v(x,t) = -\rho\cdot A\cdot\frac{d^2}{dt^2}v(x,t) \tag{2.2}$$

Equation 2.2 is describing the equilibrium of motion for a pre-stressed Euler-Bernoulli beam. The displacement in the y-direction is observed for a beam with the properties visualized in Figure 2:3. *A* is the cross-section area, *EI* is the bending stiffness and ρ is the density. The deflection of the beam is depending on where on the beam the deflection is described and when. Therefore the deformation expression in Equation 2.2 is advantageously parted into two expressions, where one part is time dependent and the other is x-axis dependent.

$$EI\cdot u(t)\cdot\frac{d^4}{dx^4}y(x) - S\cdot u(t)\cdot\frac{d^2}{dx^2}y(x) = -\rho\cdot A\cdot y(x)\cdot\frac{d^2}{dt^2}u(t) \tag{2.3}$$

How the deflection of the beam is changing during time can be described as in Equation 2.4. Since the second order derivative of the deflection (Equation 2.5) stays very similar to Equation 2.4 the cos and sin parameters disappear when Equation 2.3 is simplified into Equation 2.6.

$$u(t) = A\cdot\sin(\omega\cdot t) + B\cdot\cos(\omega\cdot t) \tag{2.4}$$

$$\frac{d^2}{dt^2}u(t) = \omega^2\cdot\left(A\cdot\sin(\omega\cdot t) + B\cdot\cos(\omega\cdot t)\right) = \omega^2\cdot u(t) \tag{2.5}$$

$$EI\cdot\frac{d^4}{dx^4}y(x) - S\cdot\frac{d^2}{dx^2}y(x) = -\rho\cdot A\cdot y(x)\cdot\omega^2 \tag{2.6}$$

From Equation 2.6 different expressions for the natural frequencies are derived depending on the end supports. It can be written generally as:

$$f_k = \kappa\cdot\frac{k}{2\cdot l}\cdot\sqrt{\frac{S}{m}} \tag{2.7}$$

The expression of κ varies due to end supports. For the case when the beam is clamped at both ends:

$$\kappa_c = 1 + \frac{2}{\beta} + \frac{1}{\beta^2}\cdot\left[4 + \frac{(k\cdot\pi)^2}{2}\right] \tag{2.8}$$

For the case when the beam is simple supported at both ends:

$$\kappa_s = \sqrt{1 + \left(\frac{k\cdot\pi}{\beta}\right)^2} \tag{2.9}$$

In both expressions *k* is the mode order and β is a parameter determined by the cable length *l*, bending stiffness *EI* and axial force *S*:

$$\beta = l \cdot \sqrt{\frac{S}{EI}} \tag{2.10}$$

Comparing Equation 2.1 to Equation 2.7 the difference is the addition of κ. κ is a parameter whose importance is increasing due to rising mode order and higher bending stiffness.

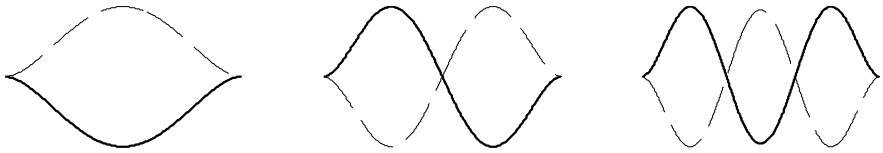

Figure 2:4 *Schematic view of the first three mode shapes of a beam or a cable with clamped ends.*

2.2.2 Central Difference Method

The central difference method is a numerical approach that can be applied to solve the difference equation Equation 2.6. The idea is to divide the cable into shorter segments with nodes at each end. By using boundary conditions the deformation of the cable nodes can be predicted with accuracy depending on the number of elements. The second and fourth derivate of *y(x)* is expressed through this numerical explicit method (explicit means that the properties of one node are expressed by using properties of other nodes).

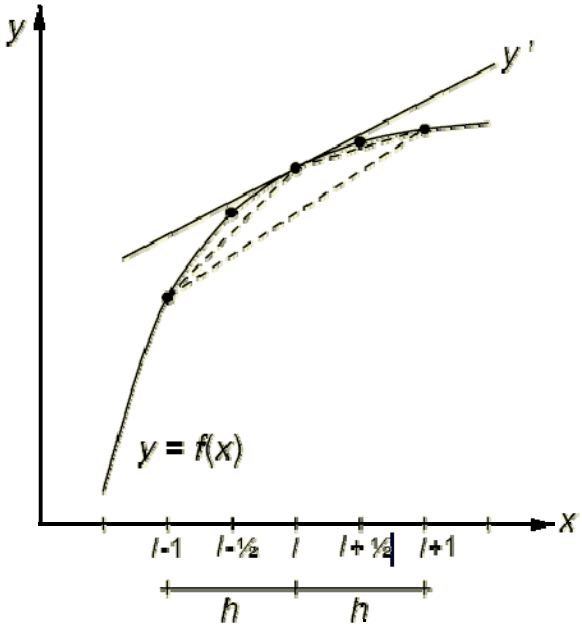

Figure 2:5 *The inclination in point x = i is described as the inclination of a straight line between two points of equal distance on each side of point x = i provides. (http://www2.mech.kth.se)*

Expressions for the first, second and fourth derivate using the parameters from Figure 2:5:

$$\frac{d}{dx} y_i(x) = \frac{y_{i+1} - y_{i-1}}{2h^2} \tag{2.11}$$

$$\frac{d^2}{dx^2} y_i(x) = \frac{y_{i+1} - 2 \cdot y_i + y_{i-1}}{h^2} \tag{2.12}$$

$$\frac{d^4}{dx^4} y_i(x) = \frac{y_{i+2} - 4\, y_{i+1} + 6 \cdot y_i - 4\, y_{i-1} + y_{i-2}}{h^4} \tag{2.13}$$

Using Equation 2.12 and 2.13 in Equation 2.6 gives:

$$EI \cdot \frac{y_{i+2} - 4\, y_{i+1} + 6 \cdot y_i - 4\, y_{i-1} + y_{i-2}}{h^4} - S \cdot \frac{y_{i+1} - 2 \cdot y_i + y_{i-1}}{h^2} = -\rho \cdot A \cdot y_i \cdot \omega^2 \tag{2.14}$$

If this is developed further using the following constants:

$$\beta_{part} = h \cdot \sqrt{\frac{S}{EI}} \tag{2.15}$$

$$k = \frac{1}{\beta_{part}^2} \tag{2.16}$$

Equation 2.14 can be expressed like this:

$$\frac{1}{\beta_{part}^2} \cdot \left(y_{i+2} - 4 \cdot y_{i+1} + 6 \cdot y_i - 4 \cdot y_{i-1} + y_{i-2}\right) - \left(y_{i+1} - 2 \cdot y_i + y_{i-1}\right) = \frac{-\rho \cdot A \cdot y_i \cdot \omega^2 \cdot h^2}{S} \tag{2.17}$$

or:

$$k \cdot y_{i+2} - (4 \cdot k + 1) \cdot y_{i+1} + (6\, k + 2) \cdot y_i - (4 \cdot k + 1) \cdot y_{i-1} + k \cdot y_{i-2} = \frac{-\rho \cdot A \cdot y_i \cdot \omega^2 \cdot h^2}{S} \tag{2.18}$$

The equations above can be treated as eigenvalue problems.

$$A \cdot Y = \frac{-\rho \cdot A \cdot \omega^2 \cdot \Delta l^2}{S} \cdot B \cdot Y \tag{2.19}$$

In Equation 2.19 the B matrix is a quadratic matrix with ones in the diagonal. The A-matrix can be described with the simplified Figure 2:6. In this figure the beam (or cable) has been divided in 10 (n) parts, with 11 (n+1) nodes. This thesis deals with cables with supported ends. Therefore the first and last rows and columns can be eliminated since y_1 and y_{n+1} are zero. Node 1 and node n+1 are the end nodes with no displacements in the transverse direction.

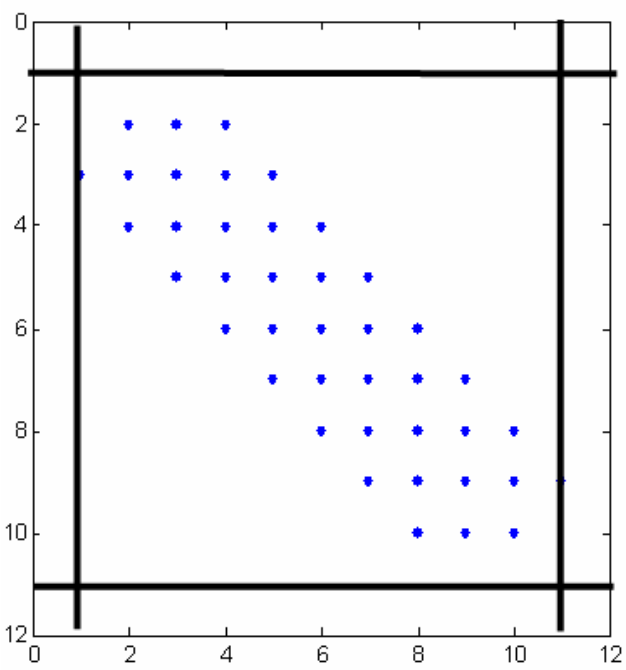

Figure 2:6 *The A matrix in the eigenvalue problem. Figure drawn by Richard Malm.*

The blue dots in one row of the matrix above correspond to:

$$k \quad -(4\cdot k+1) \quad 6\cdot k+2 \quad -(4\cdot k+1) \quad k$$

In the first row included in the matrix, the second node is described. The expression for this node is dependent on both y_1 and y_0.

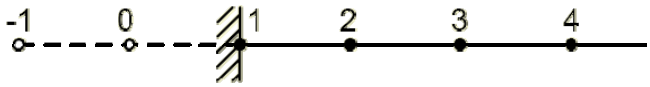

Figure 2:7 *Clamped end node. (http://www2.mech.kth.se)*

Depending on the end supports of the cable the A matrix look different. To be able to use the central difference method imaginary nodes have to be defined. For a clamped support the nodes on each side of the support are said to deform in the same way, and the following boundary conditions are valid:

$$y_1 = 0 \qquad y_0 = y_2$$

With those conditions the first row (second node) in the A matrix can be written as:

$$. \quad . \quad 7\cdot k+2 \quad -(4\cdot k+1) \quad k$$

The same argument for the last row included in the matrix, gives the reverse expression:

$$k \quad -(4\cdot k+1) \quad 7\cdot k+2 \quad . \quad .$$

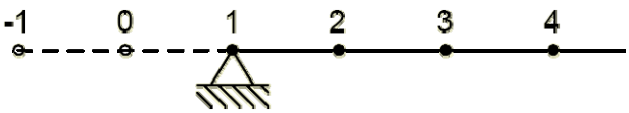

Figure 2:8 *Simple supported end node. (http://www2.mech.kth.se)*

For a simple support the boundary conditions are:

$y_0 = -y_2 \qquad y_1 = 0$

With those conditions the first row (second node) in the A matrix can be written as:

$$\begin{matrix} . & . & 5\cdot k + 2 & -(4\cdot k + 1) & k \end{matrix}$$

The same arguments for the last row included in the matrix gives the reverse expression:

$$\begin{matrix} k & -(4\cdot k + 1) & 5\cdot k + 2 & . & . \end{matrix}$$

Consequently, a cable divided into 10 parts with 11 nodes will give an A matrix with the dimension 9x9. The matrix's first and last value in the diagonal differs between 5k+2 and 7k+2 depending on the nature of the end supports. In the matrix below the constant c differs from 1 for free rotation (simple supported) to 0 for totally clamped.

$$A = \begin{bmatrix} (7-2\cdot c)\,k+2 & -(4\cdot k+1) & k & 0 & 0 & 0 & 0 & 0 & 0 \\ -(4\cdot k+1) & 6\,k+2 & -(4\cdot k+1) & k & 0 & 0 & 0 & 0 & 0 \\ k & -(4\cdot k+1) & 6\,k+2 & -(4\cdot k+1) & k & 0 & 0 & 0 & 0 \\ 0 & k & -(4\cdot k+1) & 6\,k+2 & -(4\cdot k+1) & k & 0 & 0 & 0 \\ 0 & 0 & k & -(4\cdot k+1) & 6\,k+2 & -(4\cdot k+1) & k & 0 & 0 \\ 0 & 0 & 0 & k & -(4\cdot k+1) & 6\,k+2 & -(4\cdot k+1) & k & 0 \\ 0 & 0 & 0 & 0 & k & -(4\cdot k+1) & 6\,k+2 & 0 & k \\ 0 & 0 & 0 & 0 & 0 & k & -(4\cdot k+1) & 6\,k+2 & 0 \\ 0 & 0 & 0 & 0 & 0 & 0 & k & -(4\cdot k+1) & (7-2\cdot c)\,k+2 \end{bmatrix}$$

The eigenvalue problem in Equation 2.19 can be solved using the MATLAB command:

```
C=(B\A);
[v,d]=eigs(C,np,'SM');
```

This command returns a diagonal matrix d with the value of the *np* smallest magnitude (*'SM'*) eigenvalues. The values in the diagonal correspond to:

$$\frac{-\rho\cdot A\cdot \omega^2\cdot h^2}{S}$$

ω is the natural circular frequency and can be replaced by $f_k 2\pi$.

h is the length of one part of the cable and can be replaced by l/n.

$$\frac{-\rho\cdot A\cdot\left(f_k\cdot 2\cdot\pi\right)^2\cdot\left(\frac{l}{n}\right)^2}{S} = -\kappa^2\cdot\frac{\pi^2}{n^2}$$

Consequently, from the diagonal matrix d the value of κ is derived. The columns in matrix v, also received from the *eigs*-command are the corresponding mode shapes (eigenvectors).

In Figure 2:9-Figure 2:12 the value of κ is shown due to β and end supports using the central difference method. The cable is parted into 800 elements. This fine division brings the numerical curve very close to the analytical in the diagram below. Similar diagrams are drawn for the first mode in *Några frågor aktuella för hängbroars dynamiska egenskaper,* Sundqvist

(2005). The advantage in using the central difference method is that it is easy to evaluate κ for all kinds of end supports from clamped to free with a good accuracy.

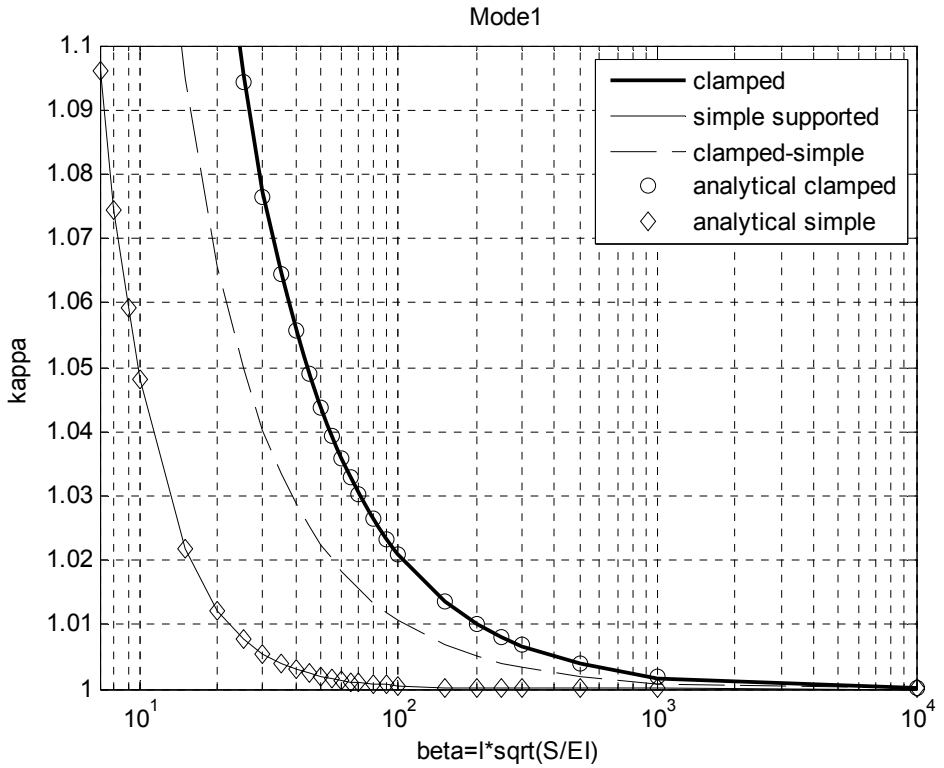

Figure 2:9 *Diagram showing how κ is depending on the end supports and β. The analytical method compared to the numerical gives no visible differences. Mode 1.*

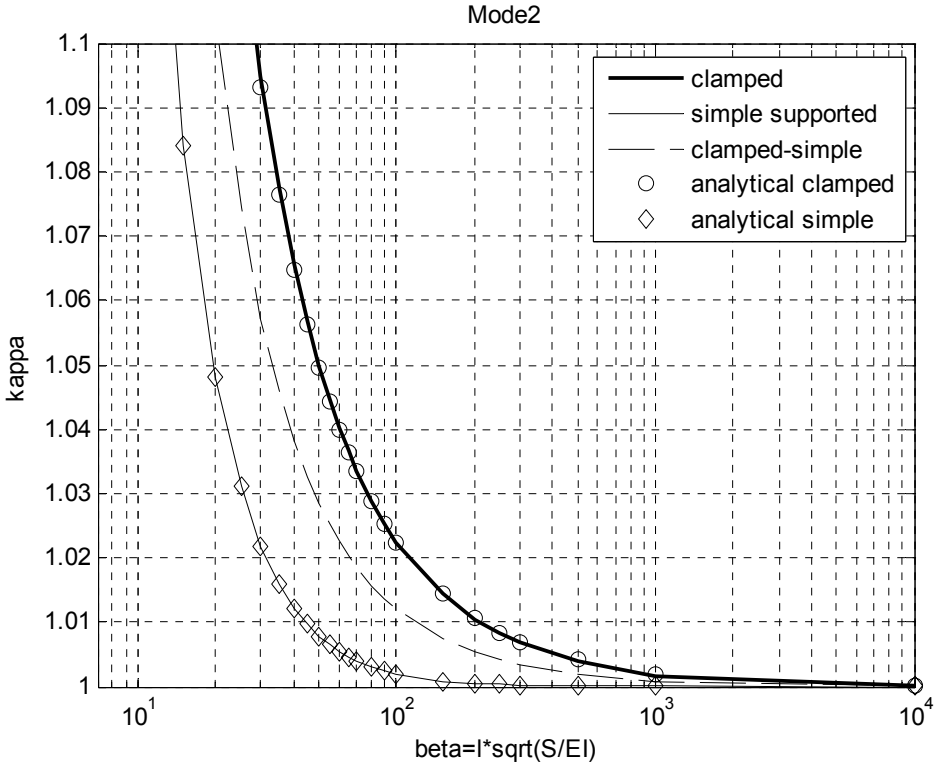

Figure 2:10 *Diagram showing how κ is depending on the end supports and β. Mode 2.*

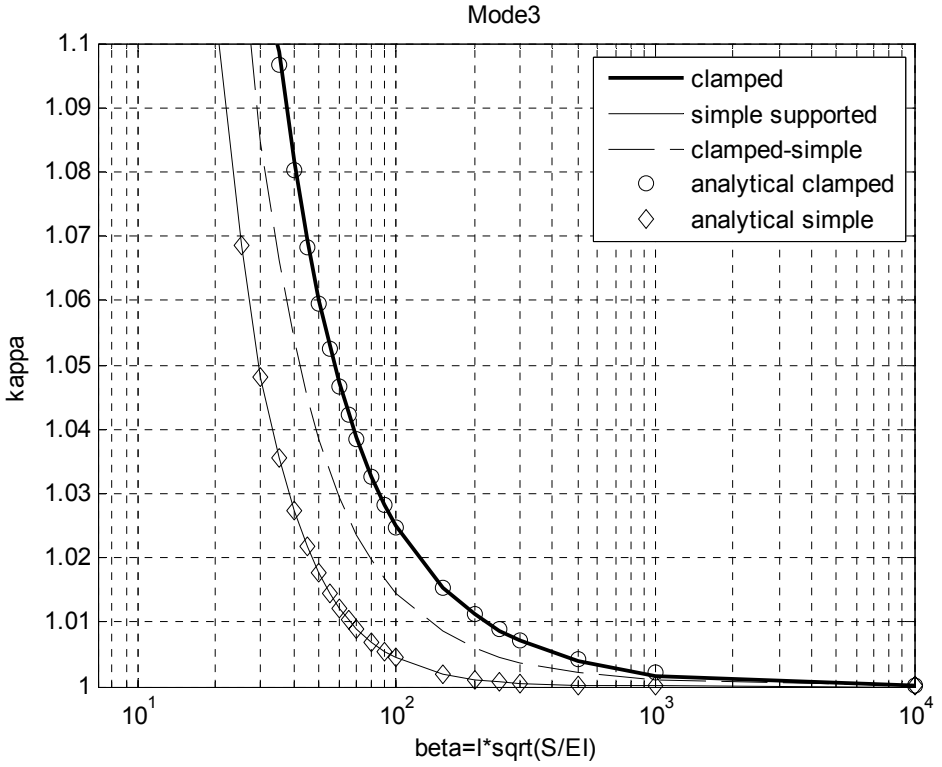

Figure 2:11 *Diagram showing how κ is depending on the end supports and β. Mode 3.*

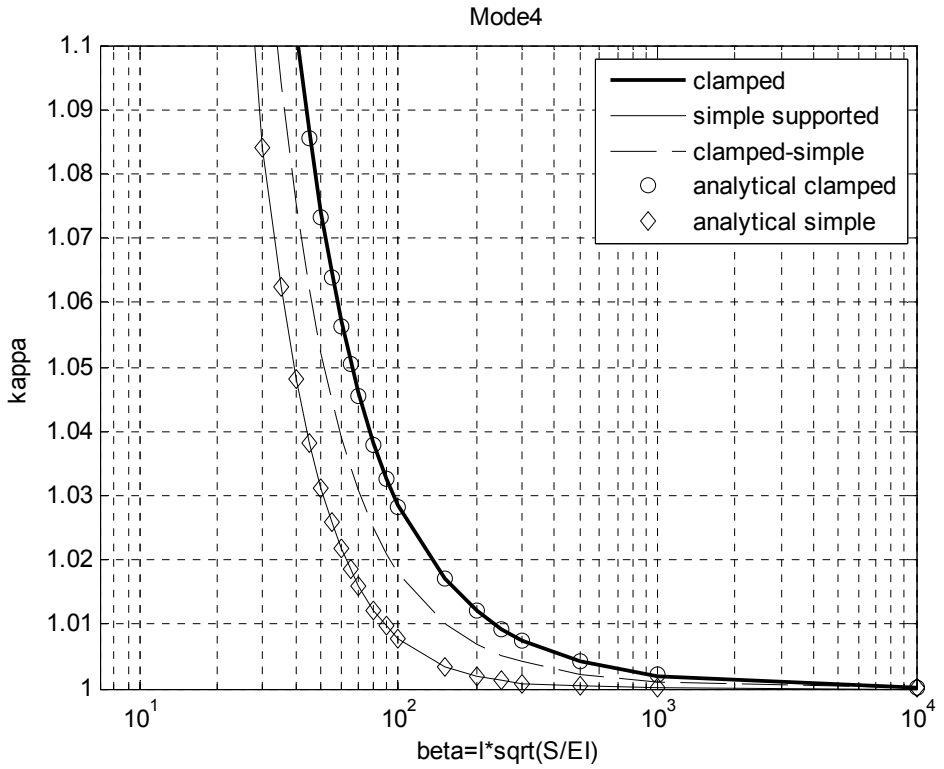

Figure 2:12 *Diagram showing how κ is depending on the end supports and β. Mode 4.*

2.3 Axial Force Evaluation

The conclusive aim in this thesis is to derive the axial force in the cables of the Älvsborg Bridge. The natural frequencies are given by measurements and signal analysis. Other properties are approximately known from the original drawings and the length of the cables has been measured. In the following section different ways to derive the axial force from the known properties are evaluated.

The axial force is extracted from Equation 2.7:

$$S = \left(\frac{2 \cdot f_k \cdot l}{k} \right)^2 \cdot \frac{m}{\kappa^2} \tag{2.20}$$

This expression involves the cable's true length l and mass per unit length m and κ. In turn, κ is depending on bending stiffness, axial force, end supports and also cable length and weight. If the end supports are assumed to be either clamped or simple supported the analytical values of κ are used (Equation 2.8 and 2.9). All the natural frequencies for the different mode orders k should give the same axial force S. Depending on how the measurements are performed it maybe possible to precise the bending stiffness that the end supports supply. Then the central difference method is well suited for the force evaluation.

There is an inaccuracy in the formulas when looking at the symmetric mode shapes (mode shapes with an odd mode order). They induce an additional force which increases the axial force in the cable. In the symmetric mode shapes this additional force gets smaller and smaller as the order increases. Therefore, the first natural frequency is the least accurately described in Equation 2.20 and is usually ignored in the evaluation of axial force in the cable Geier (2004).

The shear forces increases the more the cable bends. Therefore the Euler-Bernoulli theory, which ignores shear deformations, gets less accurate at higher mode orders.

Equation 2.20 is taking no notice of the cable sag. The cable won't be a straight line unless it is vertical. A horizontal or inclined cable will sag because of gravity as shown in Figure 2:13.

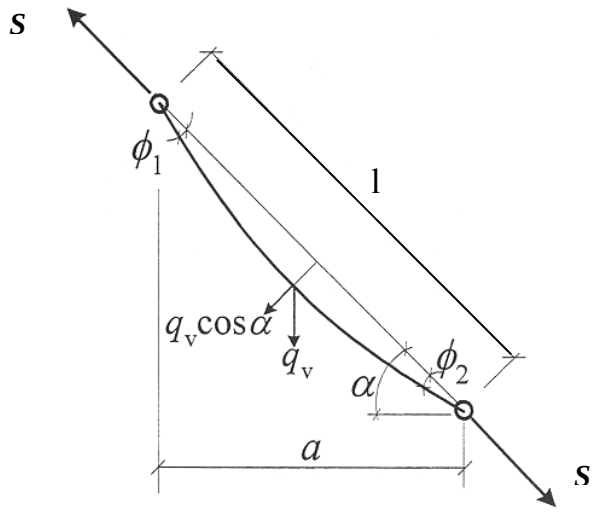

Figure 2:13 *Cable sag for a stressed cable with the inclination α. Redrawn from Sundqvist (2005).*

The sag of the cable is possible to include in the calculations by a decrease of the modulus of elasticity in the following way Lorentsen & Sundqvist (1995):

$$\frac{1}{E_i} = \frac{1}{E} + \frac{(\rho \cdot g)^2 \cdot a^2}{12 \cdot \sigma^3} \tag{2.21}$$

a = horizontal length

g = the force of gravity

ρ = density

σ = axial stress

E = modulus of elasticity

E_i = reduced modulus of elasticity with regards to the cable sag

3 Signal Analysis of a Cable

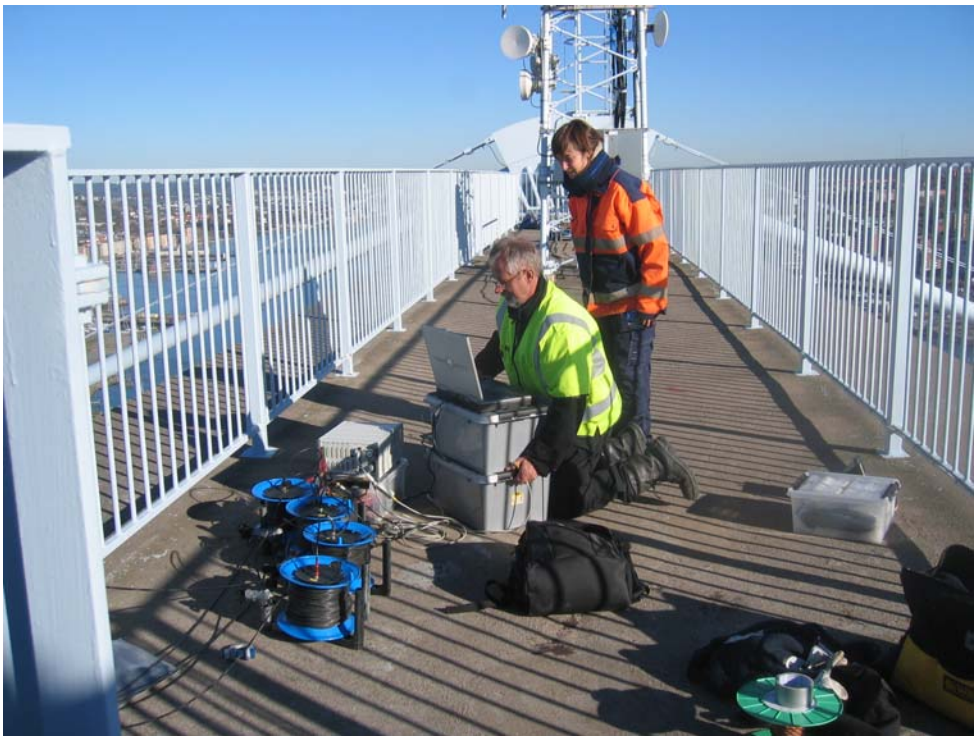

Figure 3:1 *Standing on top of the pylon at the Älvsborg Bridge. Information about the vibrations of the cable is shown on the computer screen.*

Most of the information and Figures in this chapter are taken from *The Fundamentals of Signal Analysis*, Hewett-Packard CO (1994). If other sources are used they are referred to in the text.

3.1 Different Perspectives of Dynamic Features

When evaluating the dynamic features of a cable different domains are used for the different features. The advantages of each domain are explained below.

3.1.1 The Time Domain

The time domain is a record of what happens to a parameter of the system versus time. In this thesis the system is a cable and the parameter is the acceleration of a vibrating cable in its perpendicular direction. In this domain it is possible to see the changes in movement of the cable. For example, imagine a cable at rest that is suddenly punched with a hammer. The cable will start vibrating just after the punch and then damp the vibration until it is totally still. A time record showing this event would look like the transient curve on the left in Figure 3:2.

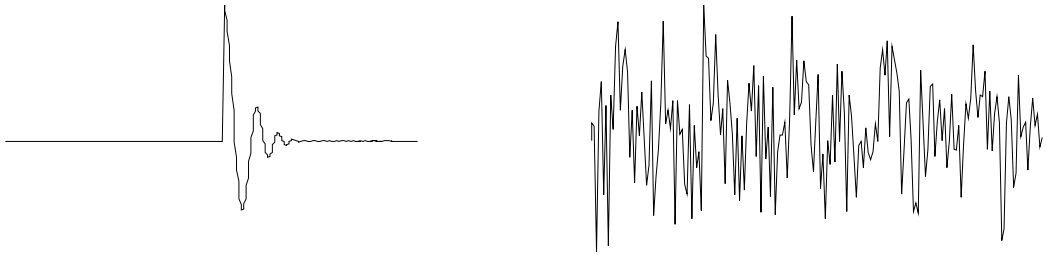

Figure 3:2 *Transient time record and a record from the measurements at the side span cable of the Älvsborg Bridge when submitted to wind and traffic loads.*

However, when monitoring cable bridges there are always forces influencing the bridge to vibrate, and it will accelerate as described in the right figure in Figure 3:2. All kinds of changes in the acceleration can be expressed as a sum of sine waves. This is true for all records, and the combination of sine waves describing the measured acceleration in the time domain is not replaceable by any other sine wave combination, it is unique. This was shown in the 19th century by Baron Jean Baptiste Fourier, therefore the name Fourier series for this mathematical description of the record.

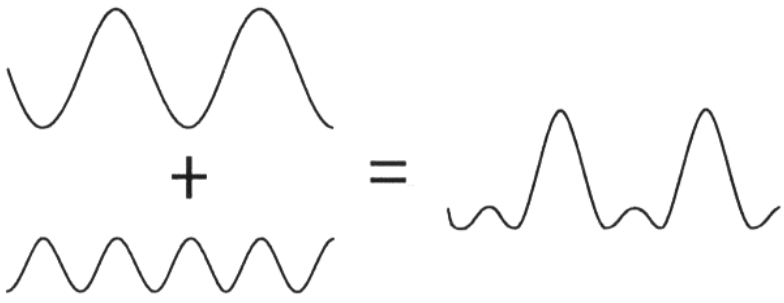

Figure 3:3 *The acceleration in the time domain can be described as the sum of many sine waves.*

3.1.2 The Frequency Domain

Accordingly, it is possible to extract sine waves from the time record. Every sine wave that is extracted has a frequency, amplitude and a phase. In the frequency domain all the sine waves in the Fourier series are represented as a line at the corresponding frequency and with the height of the amplitude. Each such line is called a *component* of the signal. The frequency domain is called the *spectrum* of the signal. When a stay cable of a bridge is vibrating because of ambient loads, traffic and wind, the time record does not say much about the features of the cable. But when the same information is transformed into the frequency domain peaks will show the natural frequencies of the cable. Even small signals are easily resolved in the presence of large once in this domain.

Measuring the width of the peaks gives the damping.

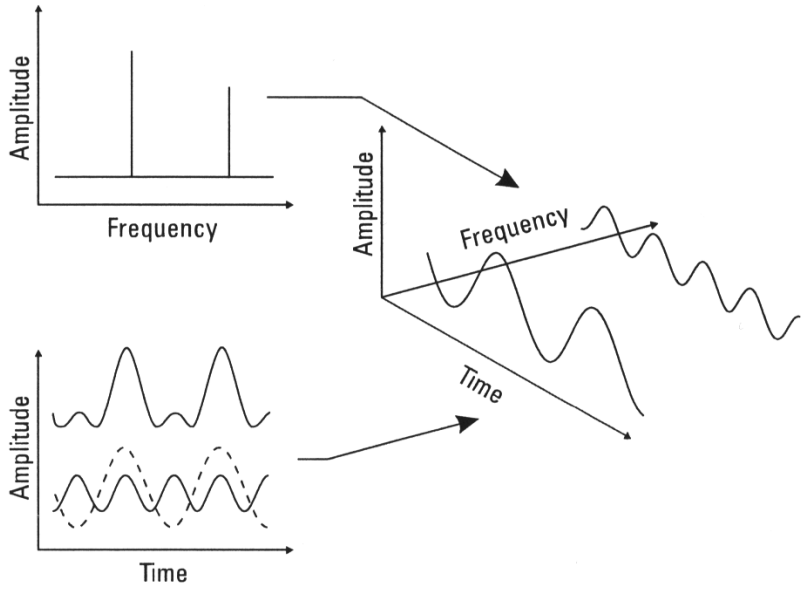

Figure 3:4 *The frequency domain on the top left. The sine waves frequency is represented by a line with the height of the amplitude.*

3.1.3 The Modal Domain

The modal domain is useful when analysing the behaviour of the cable. A vibrating cable can be moving in all directions and in different shapes at the same time. However, the vibration of the cable in one plane can be described as the sum of many *vibration modes*. A modal analysis determines the shape and magnitude of the structural deformation in each vibration mode.

3.2 Fourier Transformation

The Fourier transformation is an algorithm for transforming data from the time domain to the frequency domain. From here it is possible to do the reverse, transform the data from the frequency domain to the time domain, without loosing any information. This section refers to *Ljud- och vibrationsanalys I,* Brandt (2000).

Every periodical signal $x_p(t)$ could be formulated as a Fourier series, according to:

$$x_p(t) = \frac{a_0}{2} + \sum_{k=1}^{\infty}\left(a_k \cdot \cos\left(\frac{2\cdot\pi\cdot k}{T_p}\cdot t\right)\right) + \sum_{n=1}^{\infty}\left(b_k \cdot \sin\left(\frac{2\cdot\pi\cdot k}{T_p}\cdot t\right)\right)$$

where the coefficients a_k and b_k are formulated as:

$$a_k = \frac{2}{T_p}\cdot\int_{t_1}^{t_1+T_p} x_p(t)\cdot\cos\left(\frac{2\cdot\pi\cdot k}{T_p}\cdot t\right) dt \qquad \text{for} \qquad k = 0, 1, 2, ...$$

$$b_k = \frac{2}{T_p}\cdot\int_{t_1}^{t_1+T_p} x_p(t)\cdot\sin\left(\frac{2\cdot\pi\cdot k}{T_p}\cdot t\right) dt \qquad \text{for} \qquad k = 1, 2, 3, ...$$

The Fourier series could just as well be described as only sine waves using different constants. The true acceleration is measured with an accelerometer which transforms the information to electrical signals. To fit these signals to the computer technology they are digitalized. Thus, the time record consists of a number of equally spaced acceleration values and not a continuous curve. This is called the discrete Fourier transform. In the formulas X(k) stands for the frequency and x(k) for the acceleration.

$$X(k) = \sum_{n=0}^{N-1}\left(x(n\cdot\Delta t)\cdot e^{\frac{-j\cdot 2\pi\cdot k\cdot n}{N}}\right) \qquad \text{for} \qquad k = 0, 1, 2, ..., N-1$$

And reversely:

$$x(n\cdot\Delta t) = \frac{1}{N}\cdot\sum_{n=0}^{N-1}\left(X(k)\cdot e^{\frac{j\cdot 2\pi\cdot k\cdot n}{N}}\right) \qquad \text{for} \qquad n = 0, 1, 2, ..., N-1$$

If there are N equally spaced samples in the time domain, it becomes N/2 equally spaced lines in the frequency spectrum, but every line in the spectrum contains two pieces of information, phase and amplitude.

There are different definitions of the discrete Fourier transform. In this thesis the MATLAB Fast Fourier transformation fft.m has been used together with the function egenFFT, (A. Andersson).

```
function Y=egenFFT(rate,X)      %Converts accelerations to freqencies
y=fft(X);                       %X is the acceleration signal with
sampling frequency
                                %rate (samples/s).
N=length(X); T=N/rate;          %T is the period of the record.
f_max=rate/2; delta_f=1/T;      %Only half the spectrum is used since it
                                %is
                                %mirror-inverted
f=0:delta_f:f_max-delta_f;      %Starts at 0 Hz. To get the same amount of
                                %values as for the amplitude.
m=abs(y(1:floor((N)/2))); m(1)=0; %Abs to get rid of the imaginary part.
Y=[f',m];
```

3.3 Sampling Frequency

The measured data will never represent the real world exact because of the time gap between the samples. But it can get very close to ideal depending on how close together the samples are placed; this is called the sampling frequency.

Lower frequencies demand a longer time record to include a sufficient number of cycles. 500-1000 cycles are recommended for a good accuracy in the frequencies (A. Andersson).

The maximum frequency f_{max} that can be measured is half the sampling frequency due to the Fourier transformation. But because of the aliasing phenomena explained in the next section no frequencies less than $0.8 \cdot f_{max}$ is used.

$$f_{max} = \frac{N}{2} \cdot \frac{1}{\text{PeriodofTimeRecord}}$$

3.4 Aliasing

When using the FFT it is important to be aware of what could go wrong. Some undesirable characteristics can show up in the spectrum because of the properties of the FFT. If the sampling rate is too fast or too slow the signal input could be misunderstood. In Figure 3:5 the circles show the acceleration samples that the time recording with a sampling frequency of 12.5 Hz catch up from the real vibration of 11.35 Hz. The samples could just as well belong to a sine wave with the frequency of 1.15 Hz. The sampling frequency and the actual frequency are said to alias if their difference falls in the frequency range of interest. Consequently, the alias frequency does not exist in the real signal but will show up in the frequency domain.

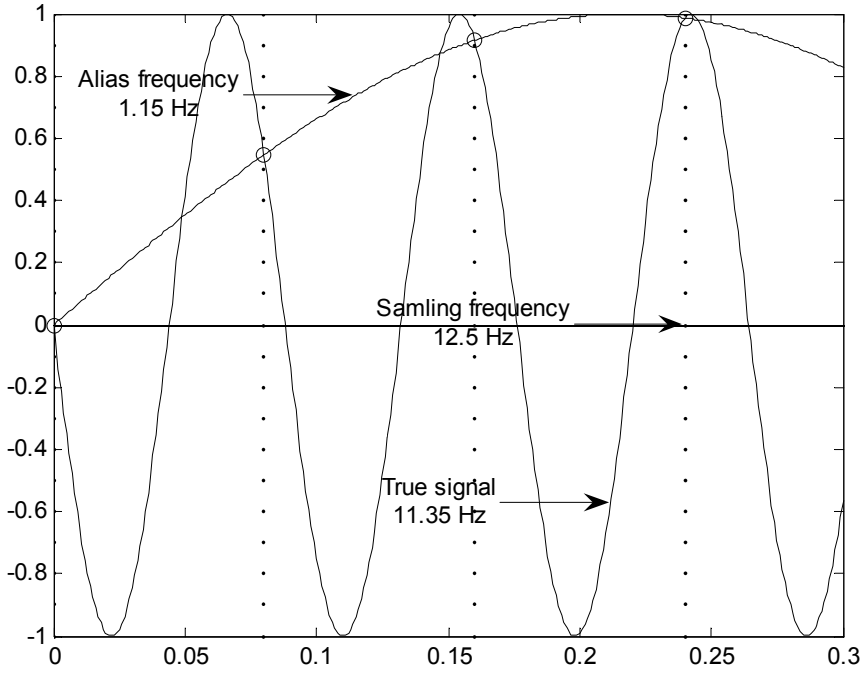

Figure 3:5 *The actual acceleration, true signal, is recorded in the time domain with the sampling frequency 12.5 Hz. The alias frequency is the sampling frequency*

minus the true signal and is not desired in the frequency domain. Redrawn from Hottinger Baldwin Messtechnik, Ambrosch (2005).

It is possible to solve the aliasing problem by sampling at more than twice the highest frequency of the input, as shown in Figure 3:6. But in bridge monitoring all kinds of frequencies are emitted, even though not of interest. Therefore a low pass filter should be used to limit the input frequency range. This filter is also called an anti-aliasing filter.

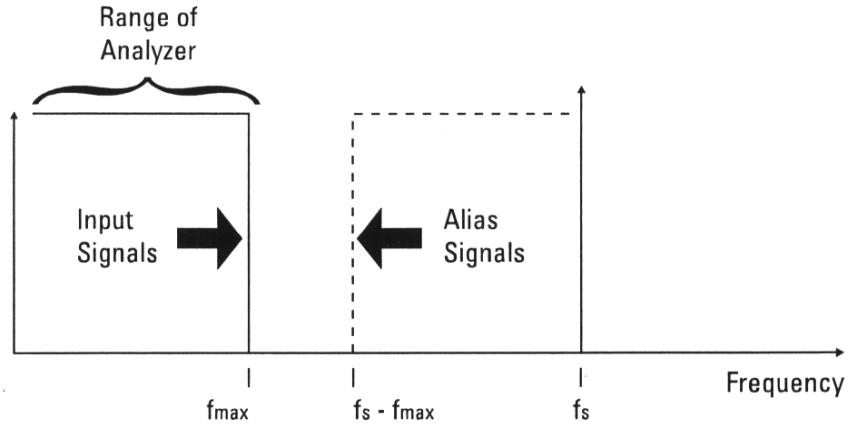

Figure 3:6 *With a sampling frequency twice as high as the maximum frequency of the structure the aliasing problem is solved. Unfortunately there are few cases when the maximum frequencies are known and finite.*

The idea of an anti-aliasing filter is that the frequencies larger than a certain value are not coming through. The filter is not working perfectly. To get a good filtering effect it is recommended to sample at 2.5 to 4 times the maximum desired input frequency with a cut-off filter must be less than 50 % (Ambrosch (2005)).

3.5 Leakage and Windowing

The time record of the accelerations will always be finite, but the FFT algorithm assume that the accelerations go on forever. This is done by letting the time record repeat itself throughout time. In Figure 3:7 the problems with this repetition is shown.

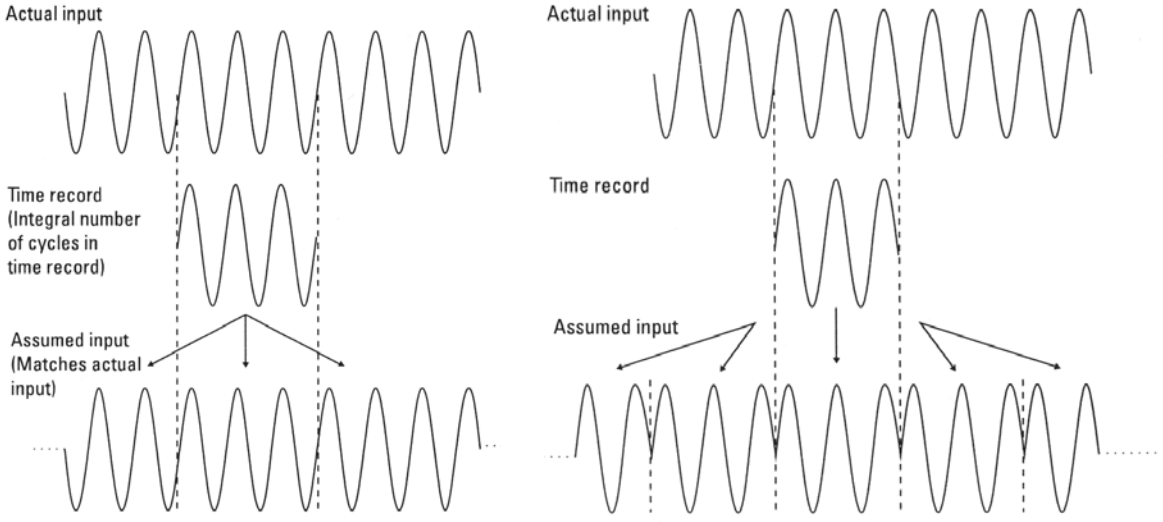

Figure 3:7 *The difference in the assumed input signal depending on weather the time record is a full number of periods or not.*

If a frequency spectrum should be drawn from the two assumed inputs above, the left one would give nice peaks at the correct frequencies, whereas the right input would give lots of other frequencies. The real peak might show but the *leakage* will hide the surrounding frequencies if they are too low in there amplitude.

To solve the problems with leakage something called windowing is used. This method ignores the ends and concentrates on the middle of the time record. In that way it is possible to reduce the unwanted frequencies from the repetition of the time record, see Figure 3:8.

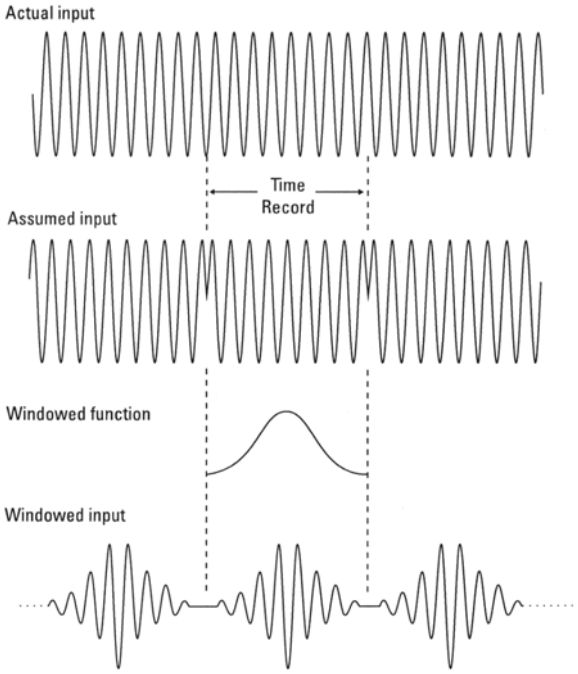

Figure 3:8 *The time record can be scaled with a windowing function to get the right frequencies at the end.*

The most common windowing function is the Hanning window. What it does is to multiply the ends with zero and keep it large at the middle.

If the input is transient because of excitation of the cable there is no need for windowing since the input already is close to zero at the ends of the time record. The windowing function applied in this thesis looks as follows:

$$\mathrm{Acc}_{\mathrm{window}} = \frac{1}{2}\cdot\left(1+\cos\left(2\cdot\pi\cdot\frac{t}{t_{tot}}-\pi\right)\right)\cdot\left(\mathrm{Acc}_{\mathrm{measured}}-\frac{\sum \mathrm{Acc}_{\mathrm{measured}}}{n}\right)$$

Here t_{tot} is the total time of the record and n is the number of samples. Windowing affect the width of the frequency peaks which makes it inapplicable for damping assessment.

4 Field Measurements at the Älvsborg Bridge

Figure 4:1 *Mounting data cables and acceleration sensors to the side span cable.*

4.1 Introduction

The number of suspension bridges and stay cable bridges has escalated during the last century (Sundqvist (1995)). There is an interest in knowing how these bridges are maintained and how they distribute their forces, for scientific reasons as well as safety control of the bridges. The pre-stressed cables are the elements that characterises these bridges. One way to determine the forces in those elements is to apply vibration monitoring methods. This method is also applied to assess the dynamical characteristics of a whole structure. In Wenzel & Geier (2002), the reasons for health monitoring are described and an historical aspect of the assessment of the dynamics of structures is presented. In the same report some of the more spectacular bridge failures due to their dynamic behaviour are discussed. For more state-of-the-art information on the topic the site www.samco.org is recommended.

The field measurements presented in this thesis took place during one week in October 2005. The objectives are to receive parameters of the Älvsborg Bridge for verification of the classification by Ramböll. There is a focus on the side span cables susceptibility for vibrations but also the modes of the pylons and the global modes of the bridge, although presented in less detail. In addition, all the strands in one splay chamber were monitored in order to see if the sum of the strand forces is equal to the main cable force. Since there are varying degrees of accuracy of the properties of the strands and cables we had expectations that this vast number of data could decrease the uncertainty in the final result.

During the field studies at the Älvsborg Bridge, KTH worked close to the Swedish road administration that was responsible for the closure of the roadway to provide a safe working area.

4.2 Equipment

When measuring the oscillation of the cables, acceleration sensors are used. These sensors are sensitive to movement in one direction. Therefore it is important to place them at the right angel. The sensor is attached to a V-shaped metal plate to easily place it perpendicular to the cable. The sensors are piezo-electric Si-Flex^{TM} accelerometers. They consist of a proof mass between two electrode wafers places in a vacuum package. The mass moves if the cable moves and the sensor emits a voltage signal proportional to the acceleration. This explanation is very simplified and further information can be accessed at the product's website (http://www.colibrys.com).

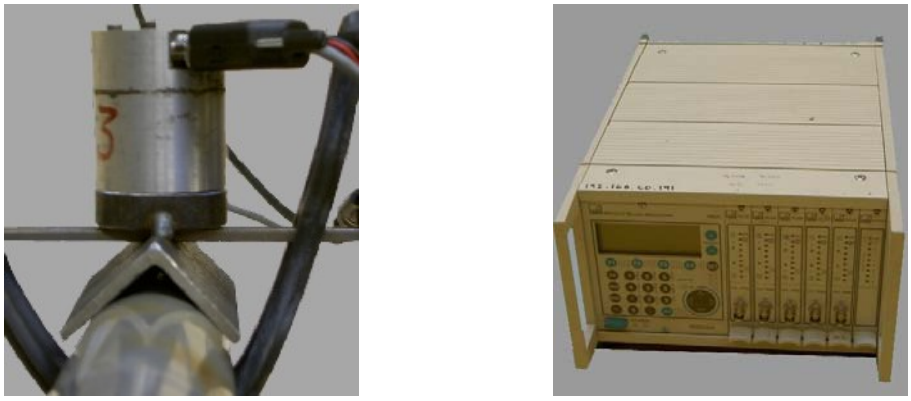

Figure 4:2 *The equipment used at the Älvsborg Bridge. Picture of the acceleration sensor on the left and the digitization system on the right.*

The data from the sensors are recorded to a computer, connected through data cables. There is a A/D converter between the computer and the acceleration sensor where one data cable from

each sensor is connected. Here the analogues (electrical) data is transformed into digital data. This is also were the cut-off filter is applied, see Section 3.4.

At the monitoring of the Älvsborg Bridge the software Cat Man was used.

The Cat Man software makes it possible to view the acceleration changes while recording. The software transforms the acceleration spectrum in the time domain to the frequency domain by a Fast Fourier Transformation. The transformation is quick and it is easy to see if the results are reliable or if something has disturbed the recording. It is also possible to compare the frequency peaks from the measurements to the estimated natural frequencies at once.

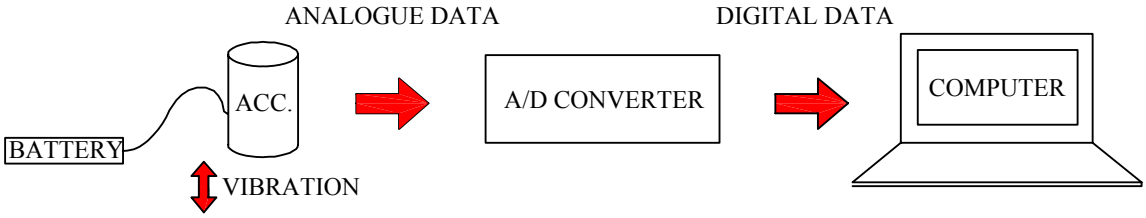

Figure 5.3 *The equipment set up. The acceleration sensor at the left is connected through data cables to the A/D converter. Digital data is recorded on the computer.*

Listing the devices:

- Battery. Power supply ± 9V.
- Acceleration sensors, Si-FlexTM SF1500S Accelerometer, +/- 3 g (http://www.appliedmems.com)
- Mounting straps for the acceleration sensors
- Digitization system, MGC plus Ambrosch (2005)
- Data cables
- Cat Man software
- Thermometer

4.3 Estimated Results

An outdoor field measurement requires some planning ahead. To be able to work efficiently it is necessary to thoroughly think through the measuring procedures, be familiar with the equipment and know what results you are expecting.

Using the Equation 2.1, describing the normal frequencies for a taut string, we get an idea of what frequency span we are looking for. This is necessary in order to know what sampling frequency to use and to quickly evaluate the measured results. In the equation the length, mass and axial force of the cable should be known. The axial force is likely to be somewhere around 65-70 MN according to a finite element model drawn up by Andreas Andersson, KTH.

In the assessment of the Älvsborg Bridge five modes are sufficient for evaluation.

	n=1	n=2	n=3	n=4	n=5
Main Cable	0,66	1,33	1,99	2,66	3,32
Strand	6,20	12,40	18,60	24,81	31,01

Table 4:1 *Estimated natural frequencies of the stay cable and the strands in the splay chamber calculated with no consideration to bending stiffness and end supports.*

4.4 The Measuring Procedure

Figure 4:3 *Mounting the sensors, cables and batteries to the stay cable. View from the south pylon.*

Two industrial climbers were engaged in the mounting of the acceleration sensors at the main cables. This is the most time consuming procedure together with the preparing and placing of the other equipment. When the system is initialised and everything set in place the recording went on smoothly. For each recording the temperature and the traffic flow was observed and documented, see APPENDIX A2. Each recording is saved to an ASCS-file with the file-name according to the list in the same appendix.

4.4.1 Side Span Cables

Five different arrangements of four acceleration sensors were monitored at the stay cables according to Figure 4:4. For every arrangement different numbers of recordings were performed, with a minimum of 3 recordings per arrangement.

Measuring frequency: 25 Hz (samples/second)

Filter: 30 % cut-off

Recording time: minimum 2 minutes

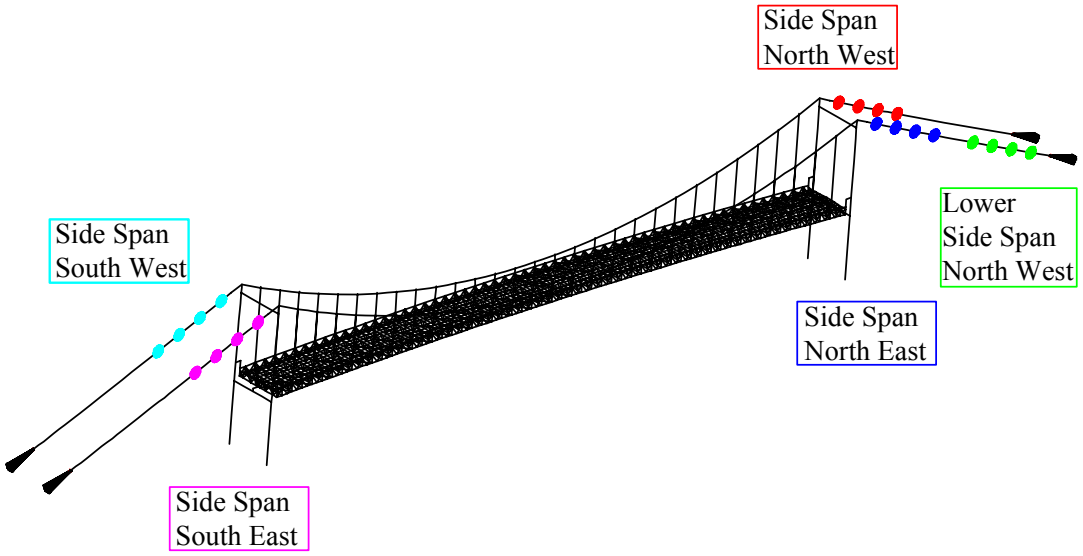

Figure 4:4 *Five different arrangements of four acceleration sensors.*

Two different methods to receive the side span cables susceptibility to vibrations were tested at the south-western and north-eastern cables.

- Excitation of the side span cable. The vibration is initiated by an applied load. A 1 ton concrete cube suspended from the middle of the cable was discharged while recording. See Figure 4:5.
- Ambient vibration testing. The stay cables accelerations were recorded when oscillating due to environmental disturbance, *ambient* loads.

These two methods give different acceleration records, see Figure 4:6. The excited monitoring result in clearer frequency spectrum as seen in Figure 4:7. However, the method is much more time consuming because of the difficulties in mounting a weight to the stay cable. Thus the ambient vibration method was considered to be sufficient enough for the north-western and south-eastern stay cables.

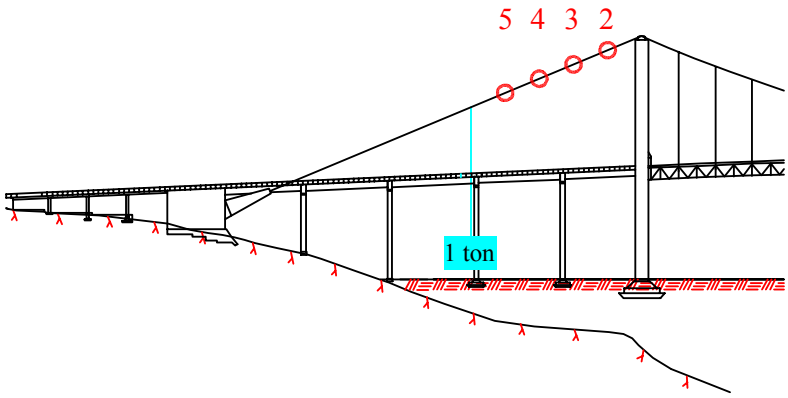

Figure 4:5 *Placement of excitation load and the measuring points. The numbers of the acceleration sensors are given. They are ordered in the same way for all upper side span measurements.*

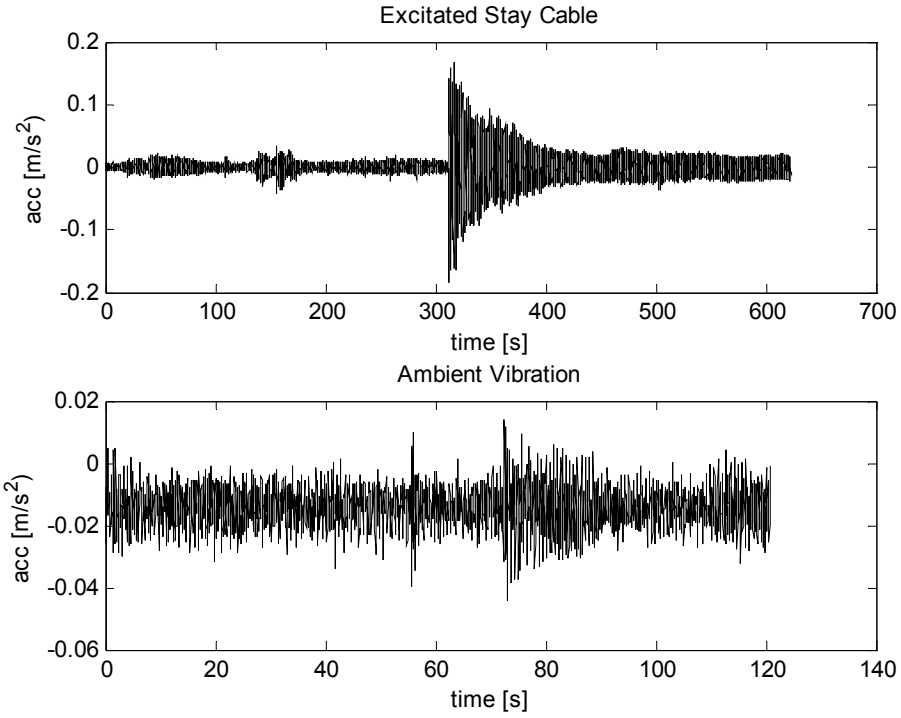

Figure 4:6 *Comparing the time domain for vibration from excited monitoring and ambient vibration monitoring.*

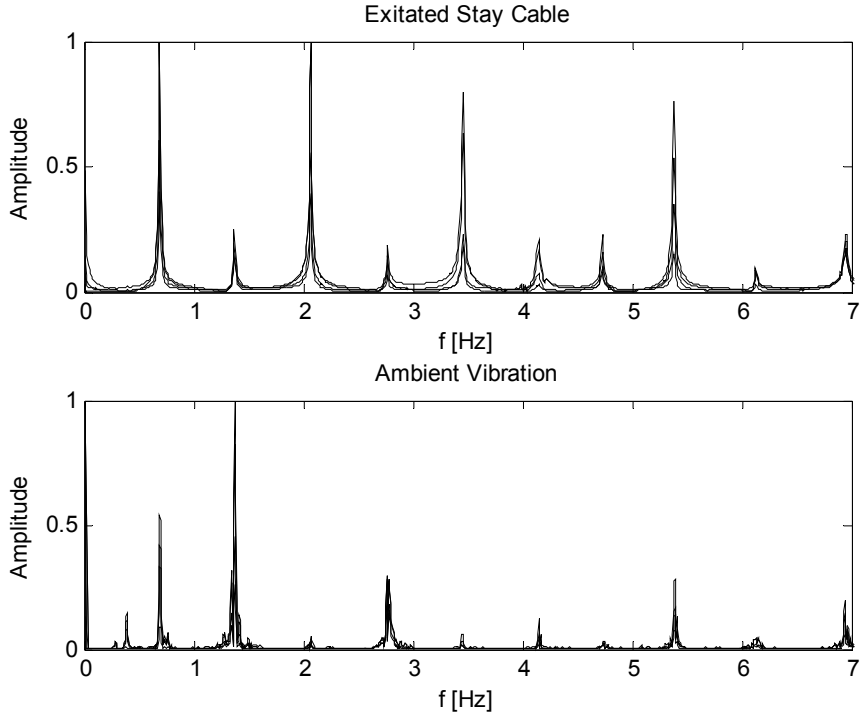

Figure 4:7 *Comparing the frequency domain for vibration from excited monitoring and ambient vibration monitoring.*

In the frequency spectrum at the top in Figure 4:7 a smaller part of the acceleration data has been used for Fourier transformation. By only choosing the part where the cable is on

influence of the excitation a smoother frequency spectrum is obtained. That is explained by the relatively small influence of traffic and wind. For ambient vibration testing the traffic and wind loads are necessary in order to set the cable in motion. These loads are contributing with frequencies that have nothing to do with the properties of the cable and result in less distinct frequency spectrum, bottom Figure 4:7.

Figure 4:8 *The acceleration sensor placed perpendicular to the stay cable*

4.4.2 Pylon

Monitoring of the south pylon was executed for both horizontal and vertical oscillation.

Measuring frequency: 25 Hz (samples/second)

Filter: 30 % cut-off

Recording time: 2 minutes

Figure 4:9 *Measurements of the pylon's susceptibility to vibration, horizontally and vertically. The photos show the placement of the acceleration sensors at a plate on the saddle.*

4.4.3 Splay Chamber

In the splay chamber the strands are quite thin. With that follows higher natural frequencies compared to the main cable. The recording is executed at 100 Hz to be able to evaluate modes one to four. All 85 strands in the north eastern splay chamber were measured.

Measuring frequency: 100 Hz (samples/second)

Filter: 30 % cut-off

Recording time: minimum 1 minute

Figure 4:10 *The splay chamber viewed from under the bridge deck.*

Figure 4:11 *The photo on the left shows Stefan Trillkott when exciting the stand with a rubber hammer. On the right Claes Kullberg is seen in front of the computer. The inclination of the splay chamber gets clear on these pictures.*

The vibration of the strand was initiated by a tap on the strand with a rubber hammer. Since this sort of monitoring gives clearer results than the ambient vibration monitoring the recording only went on for one minute. For each strand there were three runs. This means 85·1·3 = 255 minutes, four hours effective monitoring. In real life, with the mounting time of the sensors included it took more or less the double amount of time.

For two of the strands in the splay chamber measurements with three sensors in two different arrangements were executed, see Figure 4:12. Using one reference point enables mode analysis in the software MACIS/Spice.

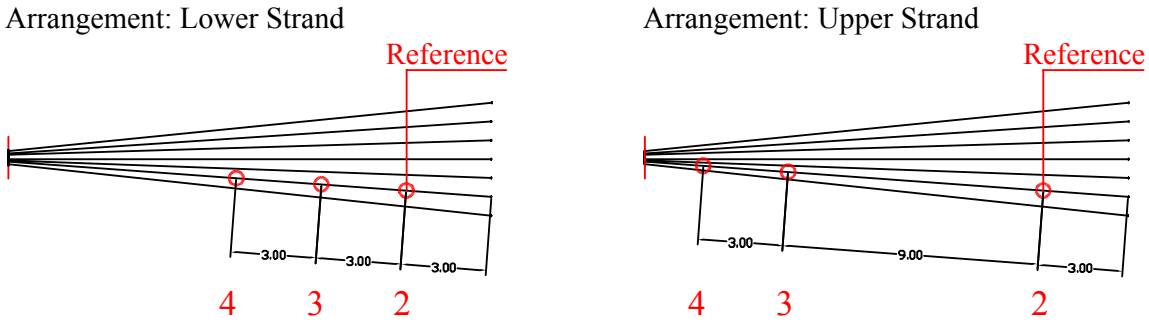

Figure 4:12 *Placements of sensors in the splay chamber for two of the strands. Many acceleration sensors are used in hope to get information about the end supports.*

4.4.4 Mid Span

Measurements in the mid span were executed in order to evaluate the global natural frequencies of the bridge.

Measuring frequency: 100 Hz (samples/second)

Filter: 30 % cut-off

Recording time: 5 minutes

Sensors were placed on the truss and on the main cable in the middle of the mid span between hanger 14 and 15. The vertical and transverse vibrations were measured.

The truss was monitored at hanger 6 for vibration in the vertical, transverse and longitudinal directions.

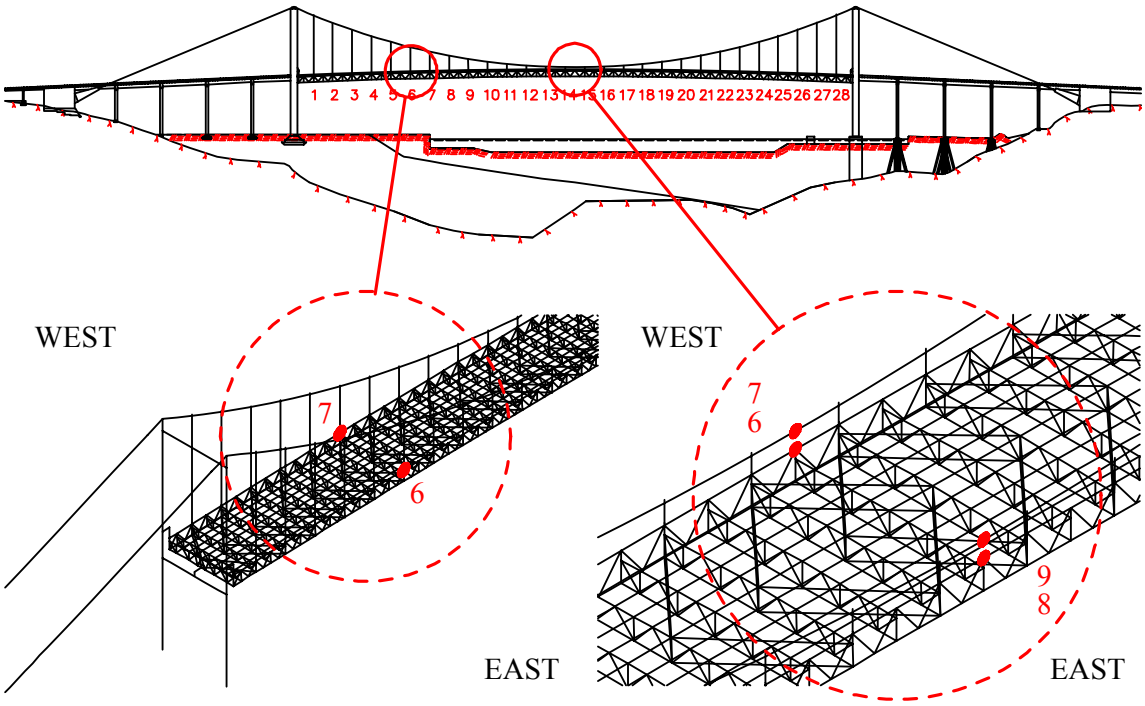

Figure 4:13 *Measuring points in the mid span.*

5 Results

Figure 5:1 *Inside the splay chamber.*

5.1 Measured Frequencies

5.1.1 Side Span Cables

The acceleration/time records received from the measurements are transformed into frequency spectra through the MATLAB built in function fft.m.

The maximum frequency in the spectra will be half the sampling frequency, 25/2 = 12.5 Hz. With a 30 % cut-off, only the frequencies less than 7.5 Hz will be clear in the spectra.

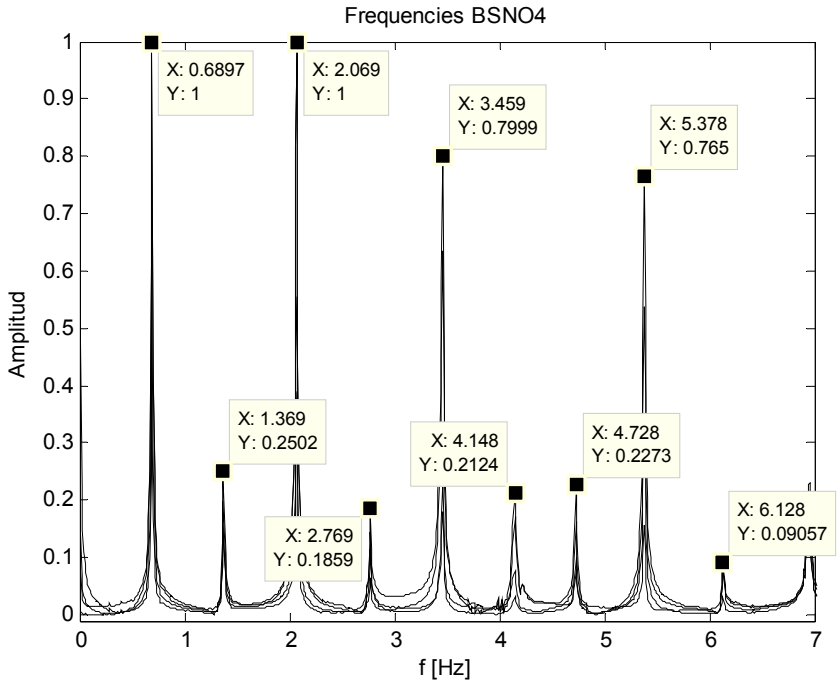

Figure 5:2 *The frequency spectrum for the north-eastern side span when excited. Results from all 4 sensors are represented.*

An average of the natural frequencies from the measurements is presented in Table 5:1. For the north-eastern side span and the south-western side span only the excited measurements are included since they give more accurate results.

For the north-western and south-eastern side spans the windowing function in section 3.5 is applied. However, the untreated record also gives a clear spectrum and the windowing function does not make any big difference. Since many measurements are analysed the peak values are received through a MATLAB function, *dat2tp*, from Lund University (http://www.maths.lth.se/matstat/wafo/). The peaks are marked with a circle in Figure 5:3.

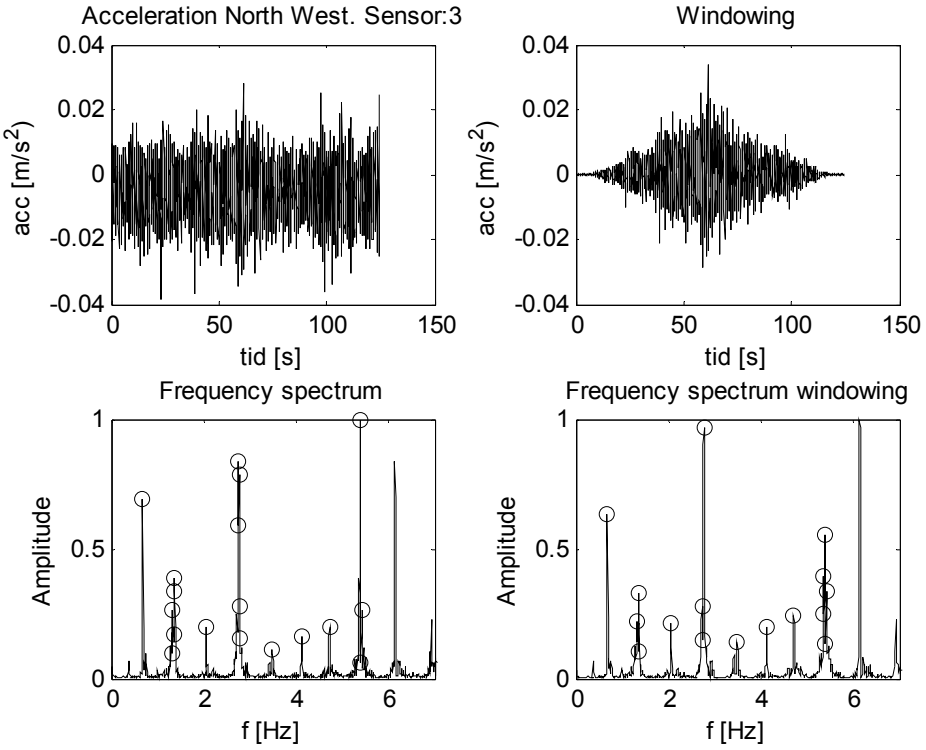

Figure 5:3 *At the top left the time record is shown for the measurements at the north-western side span cable. On the top left the record has been windowed. The lower figures show the respective frequency spectra.*

	1	2	3	4	5	6	7	8
Side span North East	0,69	1,37	2,07	2,77	3,46	4,14	4,73	5,38
Lower:	0,69	1,38	2,07	2,77	3,48	4,15	4,74	5,39
Side span North West	0,69	1,37	2,06	2,77	3,50	4,13	4,72	5,38
Side span South East	0,71	1,42	2,14	2,83	3,56	4,22	4,87	5,52
Side span South West	0,71	1,41	2,12	2,84	3,54	4,19	4,85	5,53

Table 5:1 *The frequency peaks for the five side span arrangements.*

In Table 5:1 the 8 first natural frequencies are presented. The northern cables have more or less the same values and that is also true for the southern cables.

5.1.2 Pylons

Measurements of the vertical frequencies did not give any clear results. The results for the pylons are picked out by Andreas Andersson A. Andersson. The results from these measurements are not of big interest in the assessment of the axial forces in the stay cables, and not further analysed in this report.

	1	2	3
Horizontal:	0,29	0,39	0,51

Table 5:2 *The frequency peaks for the horizontal movement in the pylon.*

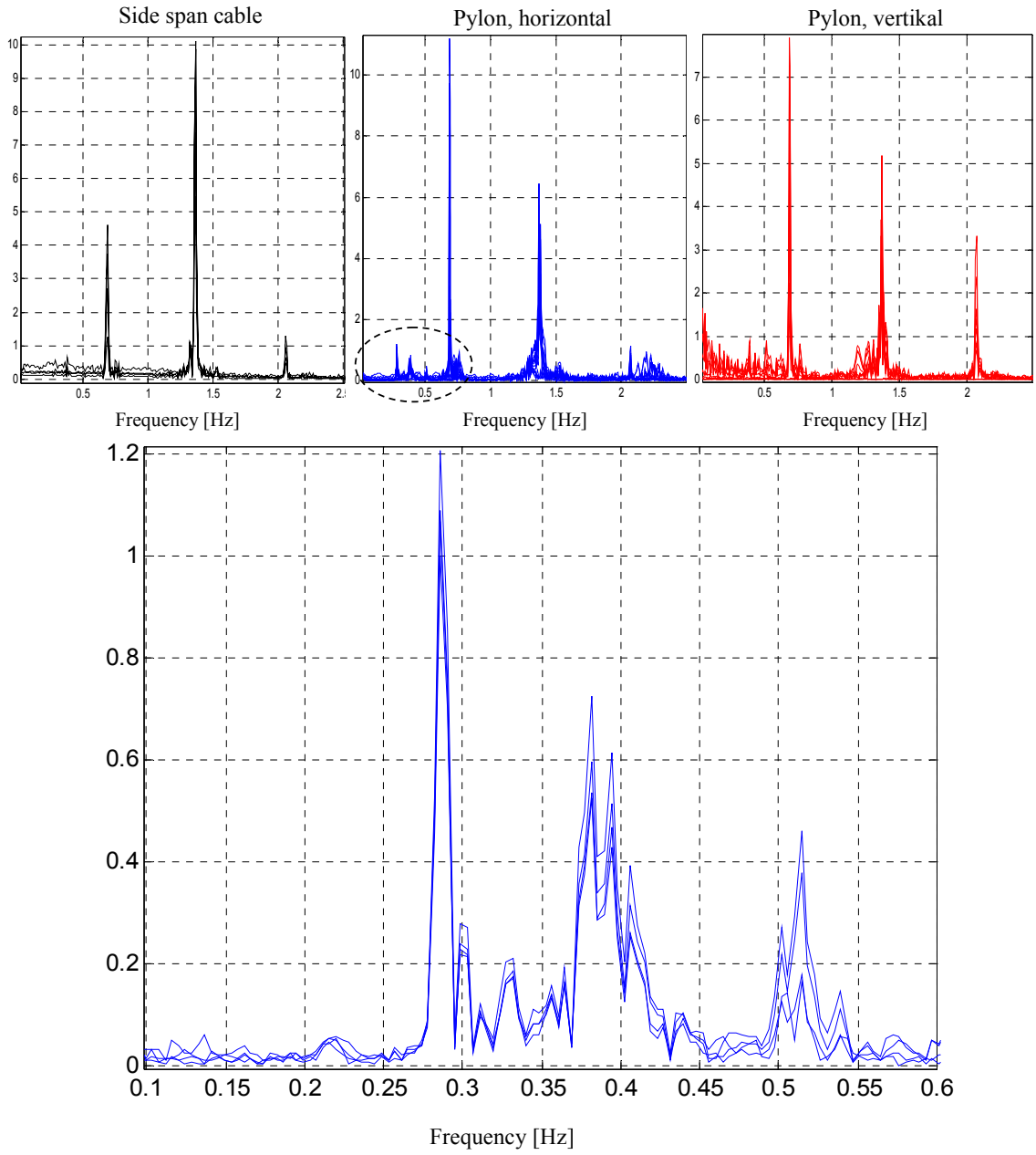

Figure 5:4 *Figure showing the frequency peaks from three measurements of the horizontal vibration and three measurements of the vertical vibration of the pylon. The natural frequencies of the side span cable are recognised as well as three other peaks in the horizontal spectrum. Modified from diagrams by Andreas Andersson.*

5.1.3 Strands in the North Eastern Splay Camber

All the 85 strands in the north eastern splay chamber were monitored. Each strand was recorded for one minute after excited with a rubber hammer. The highest frequency without any cut-off effect is 30 Hz. The fifth mode has a frequency higher than 30 Hz, plus that the placement of the acceleration sensor is unfavourable for this mode, see Figure 5:5. Therefore, only mode1-4 is used for further evaluation.

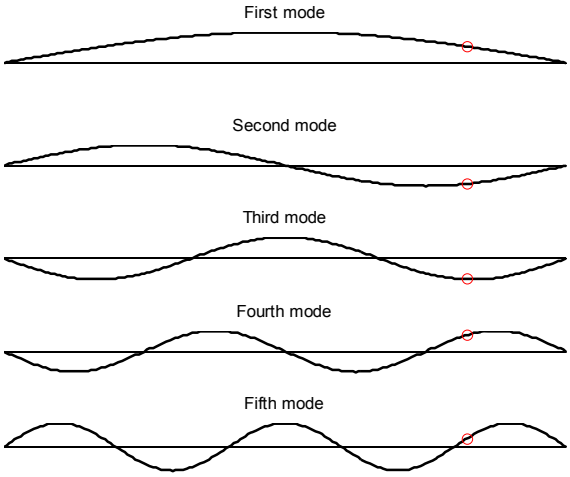

Figure 5:5 *The placement of the sensor is 3 meters from the end wall in the splay chamber. This gives nice accentuation of the peaks for the first four natural frequencies, but hardly readable peak for the fifth frequency.*

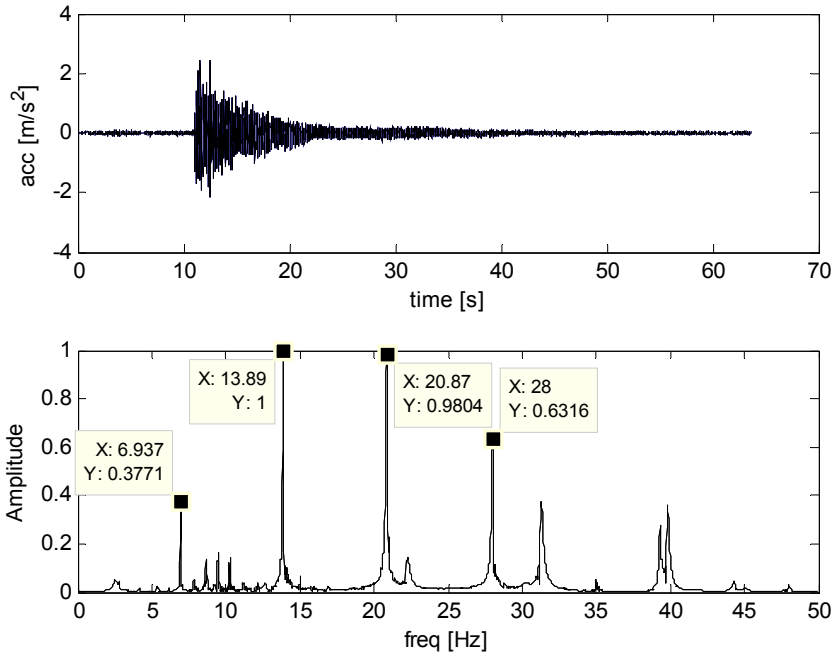

Figure 5:6 *Time and frequency domain spectra for strand 101's third run.*

To be able to increase the accuracy in the force determination strand 201 and 202 were monitored for mode analysis in hope of getting to know the true end conditions. This analysis was not completed since more time would be needed. But from a quick look with the software MACES/Spice strand 201 would be considered clamped at the lower end and free at the other. But for strand 202 the results were unclear.

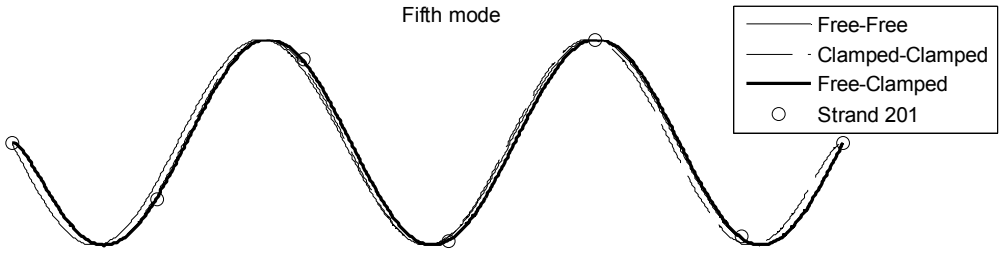

Figure 5:7 *The displacements of the measuring points at strand 201 for mode shape 5 are compared to the theoretical shapes for different boundary conditions.*

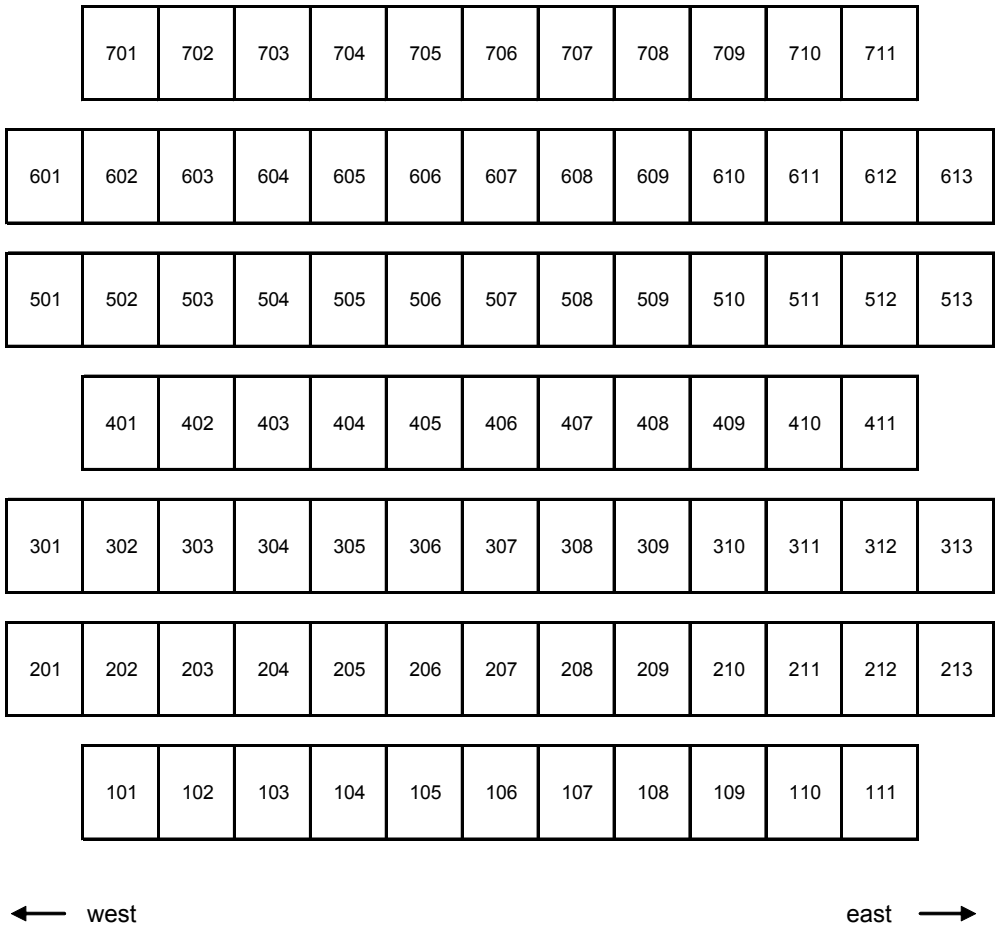

Figure 5:8 *The numbering of the strands in the splay chamber. The monitoring started at noon and continued till late the same day. Each strand was excited three times and recorded for one minute.*

Mode:	1	2	3	4	5
Strand: 101	6,93	13,84	20,86	28,00	34,96
102	6,90	13,80	20,80	28,00	35,40
103	7,24	14,49	21,70	29,00	37,20
104	6,91	13,90	20,90	28,10	35,50
105	7,08	14,15	21,40	28,73	36,22
106	6,91	13,91	20,98	28,14	35,55
107	7,08	14,15	21,23	28,48	34,90
108	6,83	13,74	20,73	27,98	35,40
109	7,16	14,40	21,65	28,89	37,47
110	6,83	13,74	20,65	27,81	35,22
111	6,91	13,82	20,90	28,06	35,47
201	6,90	13,80	20,85	28,06	35,40
202	6,98	13,95	21,04	28,29	35,48
203	6,86	13,72	20,70	27,85	35,30
204	6,93	13,86	20,92	28,05	34,80
205	6,80	13,66	20,59	27,58	34,00
206	6,86	13,79	20,79	27,91	35,24
207	6,86	13,66	20,59	27,71	34,78
208	6,86	13,72	20,72	27,91	35,31
209	6,80	13,59	20,52	27,65	35,04
210	6,93	13,92	20,92	28,11	35,11
211	6,80	13,59	20,52	27,65	35,04
212	6,93	13,92	20,99	28,25	35,71
213	6,93	13,86	20,85	28,11	35,51
301	6,80	13,52	20,39	27,45	
302	6,76	13,53	20,52	27,59	34,82
303	6,84	13,68	20,60	27,75	35,00
304	6,76	13,60	20,45	27,59	34,82
305	6,69	13,45	20,22	27,21	34,44
306	6,69	13,45	20,22	27,13	33,82
307	6,76	13,53	20,45	27,36	34,44
308	6,65	13,34	20,14	26,99	34,03
309	6,90	13,81	20,80	27,88	35,15
310	6,74	13,61	20,47	27,34	33,96
311	6,70	13,39	20,19	27,19	34,33
312	6,89	13,80	20,80	27,90	35,30
313	6,93	13,86	20,92	27,98	34,78
401	6,70	13,50	20,33	27,30	34,40
402	6,65	13,29	20,00	26,90	33,80
403	6,60	13,24	19,94	26,84	33,93
404	6,55	13,09	19,70	26,55	33,55
405	6,61	13,24	19,94	26,80	33,70
406	6,30	12,64	19,04	25,54	32,20
407	6,65	13,29	20,00	26,84	33,80
408	6,50	13,04	19,64	26,39	33,40
409	6,60	13,19	19,89	26,80	33,80
410	6,91	13,90	20,89	28,00	34,50
411	6,85	13,70	20,64	27,75	34,90

	Mode:	1	2	3	4	5
Strand:	501	6,60	13,14	19,84	26,64	33,63
	502	6,60	13,19	19,89	26,79	33,83
	503	6,80	13,59	20,49	27,60	34,78
	504	6,90	13,74	20,74	27,79	34,53
	505	6,70	13,39	20,19	27,09	34,08
	506	6,70	13,44	20,24	27,09	33,23
	507	6,65	13,29	20,04	26,94	33,90
	508	6,75	13,49	20,34	27,19	33,38
	509	6,90	13,69	20,64	27,69	34,23
	510	6,85	13,74	20,50	27,27	36,36
	511	6,65	13,34	20,09	26,99	34,10
	512	6,70	13,44	20,19	27,14	33,93
	513	6,70	13,39	20,19	27,09	33,78
	601	6,60	13,24	19,99	26,84	33,60
	602	6,50	13,04	19,59	26,09	34,78
	603	6,50	13,10	19,70	26,40	34,10
	604	6,48	12,99	19,60	26,34	32,94
	605	6,63	13,25	19,97	26,74	33,10
	606	6,84	13,71	20,68	27,76	34,35
	607	6,89	13,80	20,77	27,64	31,10
	608	6,80	13,50	20,28	27,57	34,40
	609	6,66	13,35	20,10	27,00	33,00
	610	6,57	13,18	19,85	26,50	33,45
	611	6,57	13,14	19,79	26,49	33,58
	612	6,63	13,24	19,99	26,79	33,20
	613	6,40	12,84	19,34	25,89	31,48
	701	6,49	13,00	19,60	26,30	32,10
	702	6,65	13,29	20,04	26,94	33,28
	703	6,70	13,39	20,14	26,79	32,40
	704	6,44	12,91	19,47	26,15	32,31
	705	6,72	13,46	20,27	27,07	31,95
	706	6,76	13,47	20,31	27,35	33,67
	707	6,48	12,99	19,59	26,27	31,90
	708	6,80	13,59	20,47	27,43	33,63
	709	6,40	12,79	19,31	25,95	32,31
	710	6,64	13,27	19,99	26,83	28,70
	711	6,48	12,99	19,59	26,27	32,71
	Average:	6,82	13,66	20,58	27,65	34,83
	St.Dev:	0,178	0,353	0,526	0,712	1,338

Table 5:3 *Each value in the table is the mean value of three frequency spectra. The unit is Hz.*

5.1.4 Mid Span

From a finite element model made by Andreas Andersson of the bridge it is known that the first global natural frequencies of the bridge are less than 1 Hz.

The peaks from these measurements are not very sharp; see Figure 5:9 - Figure 5:11. The spectra in the longitudinal direction did not give any clear peaks at all. Perhaps this is because of all the traffic moving in this direction. The clearest spectrum is given for the vertical frequencies where it is possible that the traffic and wind has the least impact.

		1	2	3	4
Hanger 6	Horizontal:	0,19	0,45	0,65	0,76
	Vertical:	0,22	0,39	0,50	0,76
Middle of bridge:	Horizontal:	0,51	0,65	1,01	
	Vertical:	0,29	0,39	0,51	0,77

Table 5:4 *Some of the peaks in the frequency spectra for the stiffener girder. The frequency peaks from the measurements in the middle of the bridge are picked out by Andreas Andersson.*

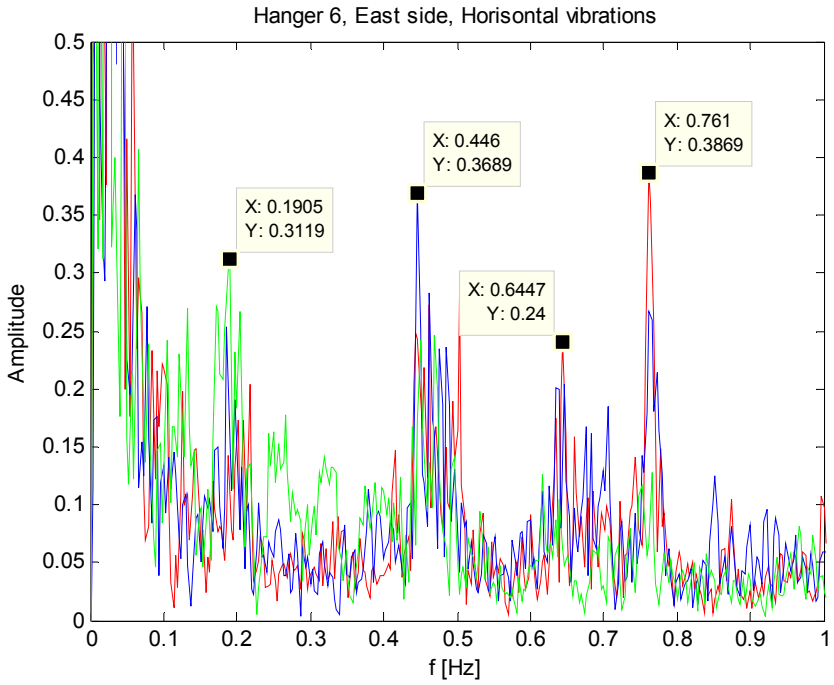

Figure 5:9 *The horizontal vibration at the east side of the bridge by hanger 6.*

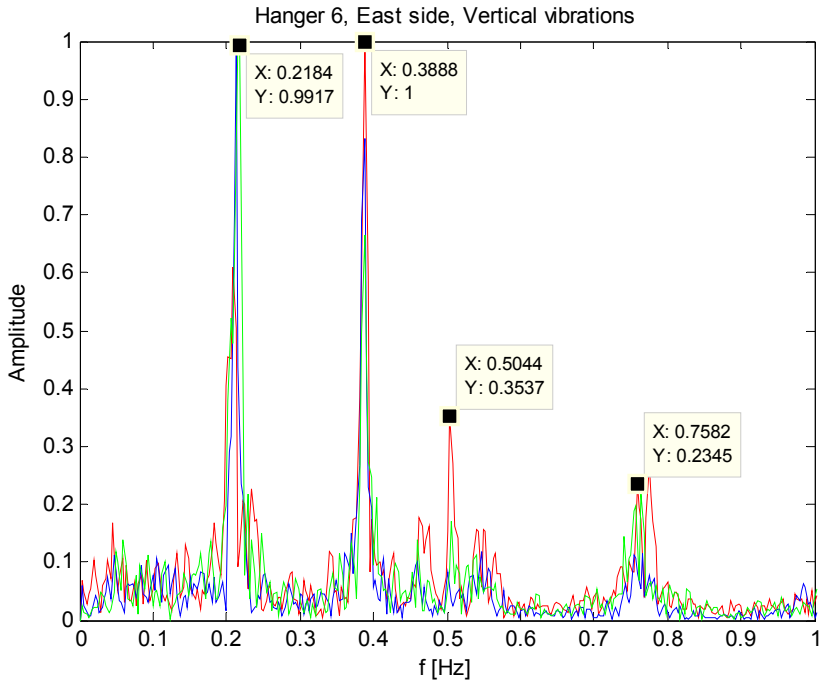

Figure 5:10 *The vertical vibration at the east side of the bridge by hanger 6.*

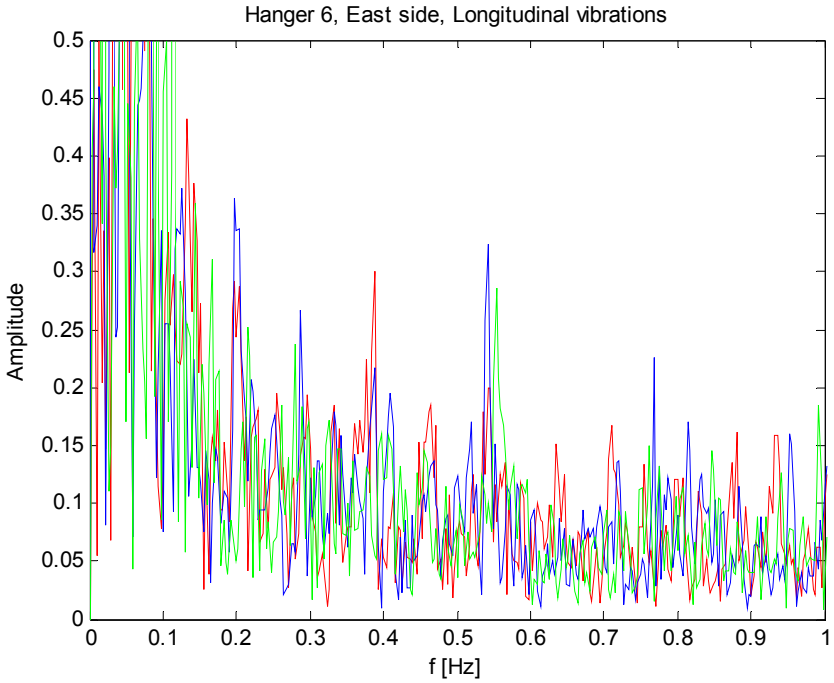

Figure 5:11 *The longitudinal vibration at the east side of the bridge by hanger 6.*

5.2 Axial Force in the Cables

The axial force in the side span cables and the strands has been calculated using Equation 2.21. The assumed values are evaluated and explained in Section 6.1.

The analytical expression that is hard to solve for other end conditions than simple supported or totally clamped. Therefore, a MATLAB code for calculations with other end conditions using the central difference method was executed and is attached in APPENDIX B1.

5.2.1 Side Span Cables

For the side span cables the saddle support is allowing the cable to rotate. At the other end it the support is neither totally clamped nor simple supported. In the calculations below the boundary conditions allow rotation at both ends to simplify the calculations. The first three natural frequencies with the assumed values below give the following axial force S in the cable:

Assumed values:

E =	163	Gpa
I =	$3{,}22*10^{9}$	mm^4
ρ =	7850	kg/m^3
m =	1534	kg/m

North span:

l =	158,6	m			
f_2 =	1,37	Hz	S_2 =	71,60	MN
f_3 =	2,07	Hz	S_3 =	71,63	MN
f_4 =	2,77	Hz	S_4 =	70,72	MN

South span:

l =	154,9	m			
f_2 =	1,41	Hz	S_2 =	72,31	MN
f_3 =	2,13	Hz	S_3 =	72,27	MN
f_4 =	2,83	Hz	S_4 =	70,24	MN

If instead the end supports are assumed to be free at the top of the pylon and clamped at the other end the axial force in the northern cables are calculated to be 69.11 MN using the first natural frequency.

5.2.2 Strands in the North Eastern Splay Camber

The length of two of the strands is known. The axial force is calculated for these two strands and for the mean strand with the average frequency values and the length 17 meters. The strands are considered clamped at both ends in the following results:

Assumed values:

E =	170	Gpa
I =	$0{,}33*10^{6}$	mm^4
ρ =	7850	kg/m^3
m =	17,2	kg/m

Strand 101:

l =	17 m				
f_2 =	13,84 Hz	S_2 =	889 291	N	
f_3 =	20,86 Hz	S_3 =	888 569	N	
f_4 =	28,00 Hz	S_4 =	887 545	N	

Strand 701

l =	17,1 m				
f_2 =	13,00 Hz	S_2 =	780 518	N	
f_3 =	19,60 Hz	S_3 =	779 229	N	
f_4 =	26,30 Hz	S_4 =	776 130	N	

Mean strand

l =	17 m				
f_2 =	13,66 Hz	S_2 =	865 392	N	
f_3 =	20,58 Hz	S_3 =	863 842	N	
f_4 =	27,65 Hz	S_4 =	864 287	N	$S_{MeanTotal}$ = 73,48 MN

To reduce the inaccuracy in the results another approach is tested. In Figure 5:12 the four first natural frequencies for all 85 strands are plotted.

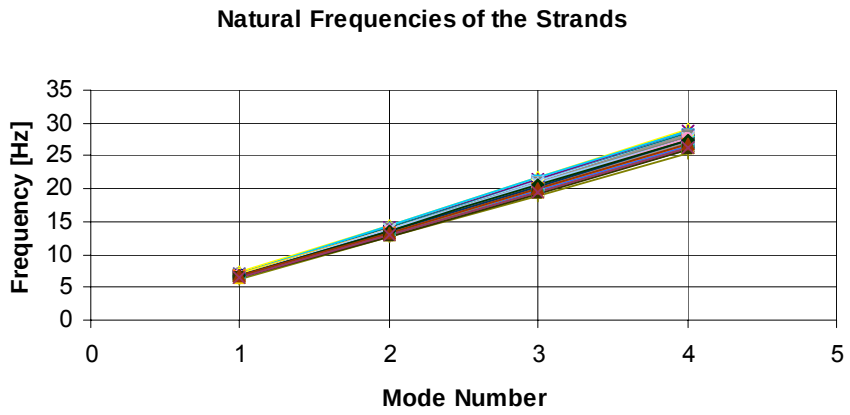

Figure 5:12 *The first four natural frequencies for all 85 strands put together.*

In Figure 5:13 the mean axial force from three recordings for the 85 strands for modes 2-4 are calculated and plotted. The value of κ is assumed to be 1 for all modes, meaning that the bending stiffness and end supports are ignored.

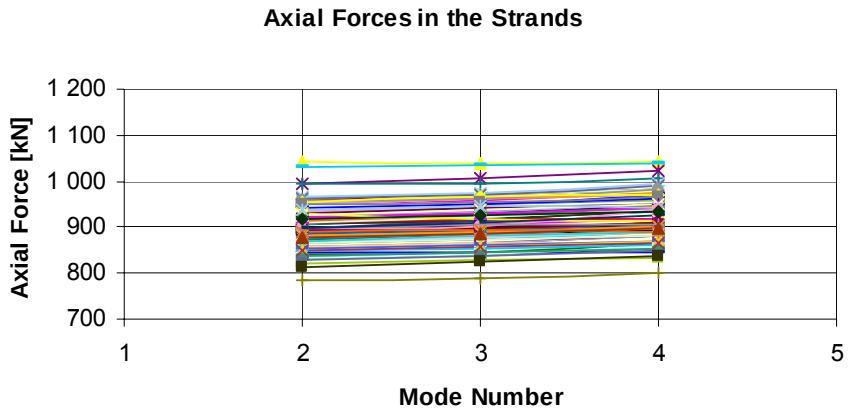

Figure 5:13 *The axial forces computed for mode 2-4. Frequencies in mode 1 and 5 are not accurate enough. Since the axial force should be the same for the different modes, we search for the κ values that would make the figure above consist of only straight lines.*

In Figure 5:13 it is seen that the force is increasing due to higher mode order. Recalling Equation 2.21 the real value of the force will be inversely proportional to the square of κ.

$$S = \left(\frac{2 \cdot f_k \cdot l}{k} \right)^2 \cdot \frac{m}{\kappa^2}$$

In Figure 5:14 the value of a constant proportional to $1/\kappa^2$ is shown for the mean strand in the splay chamber that would give the same axial force for all the mode shapes.

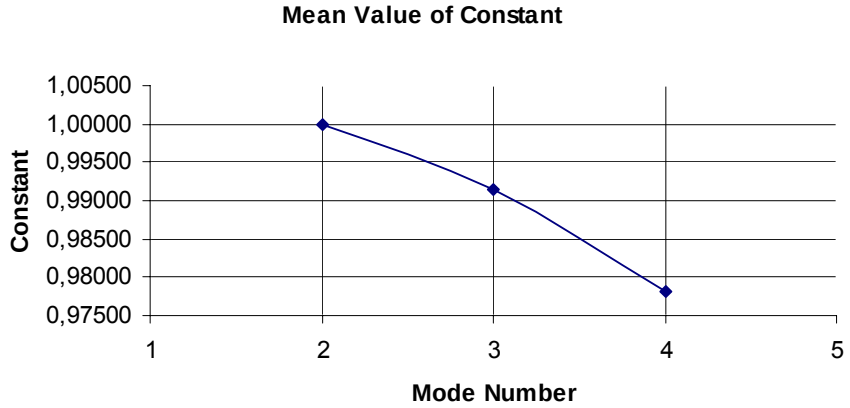

Figure 5:14 *The mean strand's axial force is the same for mode 2-4 if multiplied with the constants above.*

In the splay chamber the strands are totally clamped at the back wall, see Figure 1:11. At the other end the strand is assumed to be somewhere in-between clamped and free, see Figure 1:10. By using the MATLAB-program in APPENDIX B.2 it is possible to receive the β value with adherent κ values that will give the same axial force for the different modes. β usually depends on bending stiffness, axial force and length of the strand. Here the accuracy is increased by only letting κ depend on the boundary conditions and mode number. Using the central difference method where the constant c in matrix A on page 15 is set to be 0 at the clamped end and 0.5 at the other end.

In this way β is determined to be 72 for the mean strand.

Using the central difference method $\beta = 72$ gives:

$$\kappa_2 = 1.0318$$

$$\kappa_3 = 1.0367$$

$$\kappa_4 = 1.0435$$

This gives the mean axial force multiplied with 85 strands:

$$S_{Mean} = 72.4 \text{ MN}$$

If this value of β is correct the bending stiffness must be lower than assumed. The modulus of elasticity should be 140 GPa if the rest of the parameters are correctly assumed. If this is the case the modulus of elasticity for the main cable would also be less than assumed. An 135 GPa which gives the axial force 71.7 MN in the north spans and 72.5 MN in the south span if the supports are assumed to allow rotation and 67.2 MN and 70.1 MN if the lower support is assumed to be clamped.

6 Discussion

Figure 6:1 *The Älvsborg Bridge.*

6.1 Parametric study

The modulus of elasticity E is assumed to be 170 MPa for the strands since this is a typical value for locked coil strands according to Gimsing (1983). The sag of the cable affects the modulus of elasticity according to Equation 2.11. This effect is very small for the strand but lowers the main cables modulus to 163 GPa.

The moment of inertia, I would be $4.39 \cdot 10^5$ mm^4 for a solid strand with the same diameter as the locked coil strand in the Älvsborg Bridge. The value I have used is a bit less and originates from a reduced diameter that would give the true cross-section area of the strand, $\phi_{red}50.9$, $I = 3.3 \cdot 10^5$ mm^4.

The moment of inertia, I would be $5.55 \cdot 10^9$ mm^4 for a solid cable with the diameter ϕ580 as the main cable. In the same way as for the strands I have used a reduced diameter that would give the mass calculated by Ramböll from the original drawings, $\phi_{red}509$, $I = 3.22 \cdot 10^9$ mm^4.

The length of the strands are measured for two of them, strand 101 and 701. They are measured to be 17.0 and 17.1 respectively. From these values it is possible to calculate the length of the other strands geometrically if they are supposed to be clamped straight into the splay chamber wall. If that would be the case the minimum length would be 16.9 and the maximum length 17.1 m. But in the original drawings it is shown that the clamp arrangement allows a difference in length of ±340 mm. Since it is not known where in this span the measured lengths are, a mean length of 17.0 ± 0.6 m is assumed.

The lengths of the side span cables are 154.39 m in the south spans and 158.08 m in the north spans according to measured data from Gatubolaget (2005). I have added 0.5m since the original drawings show that the saddle is 3.2 meters wide and there is a distance of over 4 meters between the measured points closest to the saddle. The sag contributes with an elongation of 0.01 meters. The length differs from the original drawings with the lengths 153.09 and 157.065m respectively.

The mass of the strand is 17.2 kg/m according to the original drawings. The hangers had a given weight in the original drawings of 11.2 kg/m and when weighted the mass was 11.6 kg/m. That is an inaccuracy of 3.6%. I have assumed that the weight of the strands could differ with 5%.

Since the shortest recording time is 1 minute there will be a space of 0.017 Hz (1/period) between the lines in the spectra. This gives a maximum accuracy of ±0.0084 Hz for the observed frequency peak at this recording time. By using the MATLAB-function dat2tp.m the reading gets more objective.

6.1.1 Side Span Cables

For the second natural frequency of the north span the different parameters are tested for their influence on the axial force.

Variation of parameters for the north side span (simple supported at both ends):

0 < E < 205	→	S = 71,60 ± 0,82 MN
0 < I < 0,0056	→	S = 71,60 ± 0,82 MN
1461 < m < 1607	→	S = 71,60 ± 3,45 MN
157,6 < l < 159,6	→	S = 71,60 ± 0,93 MN
1,36 < f_2 < 1,38	→	S = 71,60 ± 1,06 MN

Depending on what kind of supports is assumed the force differs.

both ends simple supported	71,60 MN
clamped at one end	69,11 MN

In the figure below the axial force calculated from the five first natural frequencies are shown for all four side span cables. The first natural frequency gives the highest axial force. This could be an indication of the additional force due to symmetry in the mode shape discussed in section 2.3. The formulas used decreases in accuracy as the mode order increase. By comparing the Euler-Bernoulli theory and Timochenko theory using finite elements it could be observed that the differences are insignificant for modes between 1 and 8 A. Andersson.

In the ideal diagram all the columns representing the same side span cable would have the same height, except the slightly higher first column.

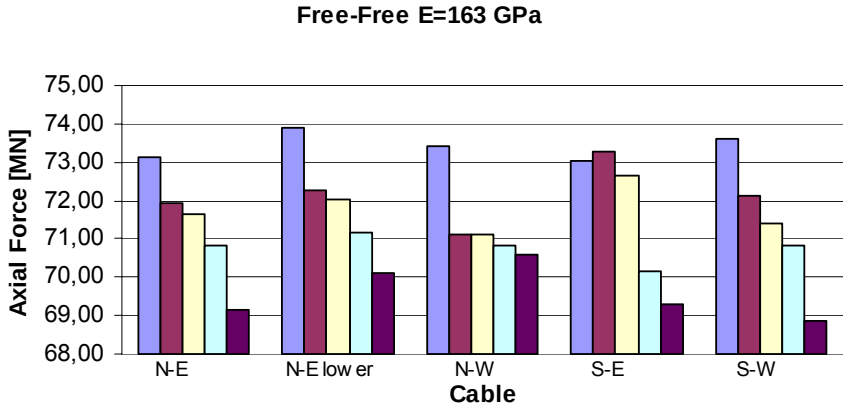

Figure 6:2 *The axial force calculated for the first five natural frequencies recorded. E = 163 GPa.*

To attain uniform columns the value of β should be somewhere between 58 and infinity, where 58 is the value obtained using the assumed size of the parameters involved. From the modulus of elasticity gained from the evaluation of the strands in the splay chamber, ≈135 GPa, β is calculated to be about 65. This makes the columns a bit more uniform, see Figure 6:3.

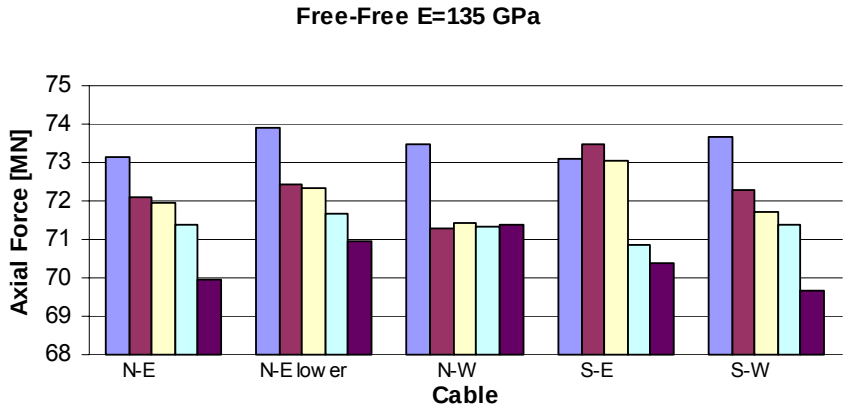

Figure 6:3 *The axial force calculated for the first five natural frequencies recorded. E = 135 GPa.*

For the main cables the saddle works as a simple support whereas the lower support is a cross between clamped and free. E = 135 GPa gives an axial force between 67.2 -71.7 MN in the north span and 70.1-72.5 MN in the south span using the assumed values for the cable mass, length and moment of inertia. The largest instability of the axial force is depending on the mass.

6.1.2 Strands

If the last approach in Section 5.2.2 is applied the accuracy is depending on the mass, the length and the measured natural frequencies of the cable. They are assumed to have certain possible intervals and together they give an inaccuracy of 14 % to the axial force. On top of that the end supports are not fully known. Even thought, the assumption should not be to far from reality. S_{CFMean} = 72.4 MN is the sum of the forces in the strands that I find most plausible after evaluation and with the information about the cables available.

6.2 Conclusions

The global frequencies read from the spectra for the horizontal and vertical vibrations are the following (the unit is Hz):

		1	2	3	4
Hanger 6	Horizontal:	0,19	0,45	0,65	0,76
	Vertical:	0,22	0,39	0,50	0,76
Middle of bridge:	Horizontal:	0,51	0,65	1,01	
	Vertical:	0,29	0,39	0,51	0,77

The frequencies are compared to the global frequencies that the finite element model made by Ramböll generates.

The axial force in the side span cables of the Älvsborg Bridge is evaluated to be 69 MN in the north span and 71 MN in the south. These values are approximate and depend on the accuracy in the assumptions about the cables. These values can be used for guidance for the model.

The north span could be compared to the sum of the axial forces in the north eastern splay chamber of 72.4 MN. There is a change in the inclination of the stands when entering the splay chamber. For force equilibrium this should be the case but not with that big difference. Converting the axial forces in the strands to there component in the same direction as the main cable approximately I get a sum of 72.3 MN instead of 72.4 MN. I have also overlooked how the temperature and amount of traffic shows in the results but without being able to see any clear relations.

In the original drawing the mean stress in the cables is assumed to be 3.973 t/cm^2 for the constant load and 4.670 t/cm^2 at the maximum traffic load. This is equivalent to an axial force of 67.6 MN and 93.4 MN. The ultimate axial force of the cable is more than 260 MN.

The natural frequencies of the side span cables could also be identified in the strand spectra and the pylon spectra. For future measurements this knowledge could simplify the procedure considerably.

The hangers are according to Ramböll, the part of interest at the moment. Their end conditions are hard to understand and therefore a difficulty in the finite element modelling. According to Claus at Ramböll these boundary conditions are crucial for the fatigue resistance of the hangers. KTH are going to do additional measurements in year 2006 in order to determine the shape of the vibration modes. To enable a good evaluation of the end conditions many measuring points with precise placements and a high sampling frequency should be applied.

REFERENCES

BIBLIOGRAPHY:

Ambrosch, M. *Digital measurement data acquisition*, Components part 2, Hottinger Baldwin Messtechnik, 2005

Asplund, C.O. *Theories applied in the design of the Älvsborg suspension bridge*, Chalmers Tekniska Högskola, Göteborg 1966

Brandt, A. *Ljud- och Vibrationsanalys I*, Blekinge Tekniska Högskola, SAVEN, 2000

Geier, R. *Evolution of Stay Cable Monitoring Using Ambient Vibration*, 2004

Gimsing, N. J. *Cable Supported Bridges*, John Wiley & Sons, 1983

Hewett-Packard CO *The Fundamentals of Signal Analysis*, Application Note 243, 1994

Lorentsen, M., Sundqvist, H. *Hängkonstruktioner*, Kompendium i Brobyggnad, KTH, fifth edition, 1995

Samuelsson, A. *Brottlastberäkning av Älvsborgsbros tornben*, Nordisk betong, 1966:4

Sundqvist, H. *Några frågor aktuella för hängbroars dynamiska egenskaper*, KTH, 2005

Sundqvist, H. *Infrastruktur konstruktioner*, TRITA-BKN, Rapport 13, ISSN 1103-4289, Brobyggnad 1995

Weaver, W., Jr., Timoshenko, S., P., Young, D., H. *Vibration Problems in Engineering*,Fifth Edition,1990

Wenzel, H., Pichler, D. *Ambient Vibration Monitoring*, Wiley, 2005

Wenzel, H., Geier, R. *State of the Art on Structural Dynamics and System Identification*, IMAC-Report-D2, 2002-02-28

Gatubolaget Elevation_Huvudkablar_Gatubolaget_til_HS.xls, June 2005

PERSONAL REFERENCES:

Andersson, A. Supervisor, Doctoral Candidate, KTH

Malm, R. Doctoral Candidate, KTH

Sundqvist, H. Professor, KTH

OTHER REFERENCES:

http://www.maths.lth.se/matstat/wafo/ Mathematical Statistics Centre for Mathematical Sciences Lund University with Lund Institute of Technology , 2006-02-28

http://www.appliedmems.com Applied MEMA, INC, 2006-03-06

http://www.colibrys.com/files/pdf/Si-Flex%201500-005%20Product%20Description.pdf 2006-03-06

http://www.vv.se/filer/publikationer/199878E.pdf General Technical Specifications for Classification calculation of road bridges, 1.1.5.1 General, Vägverket, Publ 1998, 2006-03-06

http://www2.mech.kth.se/~gunnart/BM3/F/F05-BMIII-2005.pdf 2006-03-06

APPENDIX A

A.1 People involved in the measurements of the Älvsborg Bridge:

Measuring dates:	17 October - 20 October 2005
Swedish National Road Administration (Vägverket):	Per Thunstedt
Monitoring:	Andreas Andersson (KTH)
	Alice Eklund (KTH)
	Stefan Trillkott (KTH)
	Claes Kullberg (KTH)
Mounting of equipment:	Rope Access Sverige AB

A.2 Measuring schedule:

Monday 17/10

Time:	Event:	File-name:	Temp °C:	Notes, traffic etc.:
17:55	Side span South West, traffic load	BSSV1	7	sampling 25Hz 30% cutoff, traffic photo
18:31	Side span South West, traffic load	BSSV2	6	sampling 10Hz 30% cutoff, traffic photo
18:41	Side span South West, traffic load	BSSV3	6	sampling 100Hz 30% cutoff
18:56	Side span South West, traffic load	BSSV4	5	sampling 25Hz 30% cutoff
19:00	Side span South West, traffic load	BSSV5	5	sampling 25Hz 30% cutoff
21:26	Side span South West, traffic load Exited with weight 1 ton, 3 times.	BSSV6	4	sampling 25Hz 30% cutoff

Tuesday 18/10

Time:	Event:	File-name:	Temp. °C:	Notes, traffic etc.:
14:55	Side span North West, traffic load	Bsnvtest	8	sampling 25 Hz 30% cutoff, same for all
15:05	Side span North West, traffic load	BSnvtest2	8	desturbed signal, change in current outlet.
15:52	Side span North West, traffic load	BSnv1	8	traffic photo
16:05	Side span North West, traffic load	BSnv2	8	
16:07	Side span North West, traffic load	BSnv3	8	traffic photo
16:34	Side span North East, traffic load	BSno1	7	
16:42	Side span North East, traffic load	BSno2	7	
16:57	Side span North East, traffic load	BSno3	7	
17:15	Pylon North, horisontal acc, sensor placed on saddle plate.	BSnoh1	8	
17:20	Pylon North, horisontal acc, sensor placed on saddle plate.	BSnoh2	8	
17:30	Pylon North, vertical acc, sensor placed on saddle plate.	BSnov1	8	
17:33	Pylon North, vertical acc, sensor placed on saddle plate.	BSnov2	8	
21:27	Side span North East, traffic load	BSno10min	6	test
21:43	Side span North East, traffic load + jump 2 climbers	Bsnohopp	6	
21:55	Side span North East, exiteed with weight 1 ton.	BSno4	6	
22:04	Side span North East, exiteed with weight 1 ton.	BSno5	6	desturbance: truck on bridge
22:15	Side span North East, exiteed with weight 1 ton.	BSno6	5	desturbance: truck on bridge

Wednesday 19/10

Time:	Event:	File-name:	Temp °C:	Notes, traffic etc.:
11:31	Mid span, between hanger 14 och 15, vertikal acc. Truss and main cable. Both east and west side.	MSm1v	9	sampling 100Hz, 30% cutoff same for all
11:42		MSm2v	10	much traffic, most on the eastern side
11:48		MSm3v	10	
12:13	Mid span, between hanger 14 och 15, transvers acc. Truss and main cable. Both east and west side.	MSm1h	9	sensor facing west at both sides of the bridge
12:23		MSm2h	9	
12:30		MSm3h	10	
15:55	Truss, hanger 6. sensor on both east and west side. Vertikal acc.	H6v1	13	Much traffic on west side till 16:30
16:03		H6v2	13	
16:10		H6v3	13	
16:21	Truss, hanger 6. sensor on both east and west side. Transvers acc.	H6h1	13	Sensors facing the roadway on both sides (one sensor negative)
16:29		H6h2	13	
16:34		H6h3	13	
16:46	Truss, hanger 6. sensor on both east and west side. Longitudinal acc.	H6hl1	12	Both sensors facing south.
16:55		H6hl2	12	Both sensors facing south.
17:00		H6hl3	12	Both sensors facing south.
18:08	Side span South East, traffic load	BSso1	9	Bad signal. Most traffic on west side.
18:23	Side span South East, traffic load	BSso2	9	sampling 25Hz 30% cutoff for the side span
18:30	Side span South East, traffic load	BSso3	9	
18:43	Side span South East, traffic load	BSso4	8	

Thursday 20/10

Time:	Event:	File-name:	Temp °C:	Notes, traffic etc.:
10:10	Strand 201, 3 sensors placed 3 m from each other. First one 3 m from lower wall.	201-1	9	Splay Camber North East, sampling 100HZ 30% cutoff.
10:19		201-2	9	Temperature in Splay Camber constant about 10°C
10:20		201-3	9	
10:32	Moved the upper 2 sensors 6 m up, First sensor ref.	201-4	9	
10:35		201-5	9	
10:37		201-6	9	
10:46	Strand 202, 3 sensors. First one 3 m second 12 m and third 15 m from lower wall.	202-1	9	
10:52		202-2	9	
10:54		202-3	9	
10:59	Moved the upper 2 sensors 6 m down, First sensor ref.	202-4	9	
11:03		202-5	9	
11:04		202-6	9	
11:11	One sensor, placed 3 m from lower wall.	101-1	9	
11:16	One sensor, placed 3 m from lower wall.	101-2	9	
11:17	One sensor, placed 3 m from lower wall.	101-3	9	
	This is repeated for all 85 strands. Continuouse till late night.			
11:32	Side span North East, traffic load, lower part	BSnou1	9	sampling 25Hz, 30% cutoff.
11:43	Side span North East, traffic load, lower part	BSnou2	9	sampling 25Hz, 30% cutoff.
11:49	Side span North East, traffic load, lower part	BSnou3	9	sampling 25Hz, 30% cutoff.

A.3 Frequencies in the side span cables with standard deviation:

	1	2	3	4	5	6	7	8
Side span North East	0,69	1,37	2,07	2,77	3,46	4,14	4,73	5,38
St.Dev:	0,000	0,003	0,001	0,005	0,001	0,005	0,002	0,011
Lower:	0,69	1,38	2,07	2,77	3,48	4,15	4,74	5,39
St.Dev:	0,001	0,003	0,003	0,005	0,032	0,006	0,000	0,005
Side span North West	0,69	1,37	2,06	2,77	3,50	4,13	4,72	5,38
St.Dev:	0,001	0,001	0,002	0,001	0,006	0,006	0,006	0,006
Side span South East	0,71	1,42	2,14	2,83	3,56	4,22	4,87	5,52
St.Dev:	0,005	0,010	0,005	0,013	0,017	0,017	0,023	0,005
Side span South West	0,71	1,41	2,12	2,84	3,54	4,19	4,85	5,53
St.Dev:	0,000	0,000	0,000	0,005	0,000	0,005	0,006	0,000

APPENDIX B

B.1 MATLAB Code for evaluating the value of κ from a known β and known End Conditions:

```
%% Centrala Differens Metoden
%_____________________________________________________________________________
clc,close all
T=cputime;
%% indata
%_____________________________________________________________________________
n=800;          %antal delelement
np=5;           %antal egenvärden som önskas
L=1;            %kabellängd
BETA=62.35;         %Ange beta värdet
%Inspänningsgrad
ins1=0; %0=fast,1=fri
ins2=0;
%_____________________________________________________________________________
KAPPA=zeros(length(BETA),np);       %Ska tas fram för de olika BETA-värdena
konst=1./((BETA/n).^2);
h=L/(n);                            %Längd på segmenten/elementen
x=[0:h:L]';
%% GENERERING AV MATRISER
%_____________________________________________________________________________
%_____________________________________________________________________________
%Detta sker inte för de två första och sista raderna/kolumnerna, dessa
%rader/kolumner skapas genom randvillkor
Kfast=sparse(n+1,n+1);Kfri=sparse(n+1,n+1);K=sparse(n+1,n+1);
A=sparse(n+1,n+1);
for i=3:n-1
    %Styvhetsmatris
    Kfast(i,i-2:i+2)=[konst -4*konst-1 6*konst+2  -4*konst-1 konst];
    Kfri(i,i-2:i+2)=[konst -4*konst-1 6*konst+2  -4*konst-1 konst];
    K(i,i-2:i+2)=[konst -4*konst-1 6*konst+2  -4*konst-1 konst];
end
for i=1:n+1
    %Lastmatris
    A(i,i)=1/n^2;
end
%RANDVILLKOR 1
%_____________________________________________________________________________
%Observera att jag inte ger villkor för första raden/kolumnen, eftersom
%förskjutningen är noll i första noden
%Fritt upplagd
i1=2;
Kfri(i1,i1-1:i1+2)=[0 5*konst+2  -4*konst-1 konst];
%Fast inspänd
Kfast(i1,i1-1:i1+2)=[0 7*konst+2  -4*konst-1 konst];
%Godtycklig inspännning
K(i1,i1-1:i1+2)=[0 (7-2*ins1)*konst+2  -4*konst-1 konst];
%RANDVILLKOR 2
%_____________________________________________________________________________
%Observera att jag inte ger villkor för sista raden/kolumnen, eftersom
%förskjutningen är noll i denna nod
%Fritt upplagd
in=n;
Kfri(in,in-2:in)=[konst -4*konst-1 5*konst+2];
%Fast inspänd
```

```
Kfast(in,in-2:in)=[konst -4*konst-1 7*konst+2];
%Godtycklig inspännning
K(in,in-2:in)=[konst -4*konst-1 (7-2*ins2)*konst+2];
%% BERÄKNING AV MODFORMER OCH KAPPAVÄRDEN
%observera att jag inte skickar med första och sista raden/kolumnen i
%matriserna eftersom förskjutningen är noll
Efast=(A(i1:in,i1:in))\Kfast(i1:in,i1:in);
[vfast,dfast]=eigs(Efast,np,'SM');
Efri=(A(i1:in,i1:in))\Kfri(i1:in,i1:in);
[vfri,dfri]=eigs(Efri,np,'SM');
E=(A(i1:in,i1:in))\K(i1:in,i1:in);
[v,d]=eigs(E,np,'SM');
%
%%För kappadiagram
%_____________________________________________________________________________
beta=[7 8 9 10 15 20 25 30 35 40 45 50 55 60 65 70 80 90 100 150 200 250...
    300 500 1000 10000];
kappa=zeros(length(beta),np);
kappafri=zeros(length(beta),np);
kappafast=zeros(length(beta),np);
konst2=1./((beta/n).^2);
for j=1:length(beta)
    K2=sparse(n+1,n+1);Kfast2=sparse(n+1,n+1);Kfri2=sparse(n+1,n+1);
    for i=3:n-1
        %Styvhetsmatris
        K2(i,i-2:i+2)=[konst2(j) -4*konst2(j)-1 6*konst2(j)+2...
            -4*konst2(j)-1 konst2(j)];
        Kfast2(i,i-2:i+2)=[konst2(j) -4*konst2(j)-1 6*konst2(j)+2...
            -4*konst2(j)-1 konst2(j)];
        Kfri2(i,i-2:i+2)=[konst2(j) -4*konst2(j)-1 6*konst2(j)+2...
            -4*konst2(j)-1 konst2(j)];
    end
    %Fritt upplagd
    i1=2;
    Kfri2(i1,i1-1:i1+2)=[0 5*konst2(j)+2  -4*konst2(j)-1 konst2(j)];
    in=n;
    Kfri2(in,in-2:in)=[konst2(j) -4*konst2(j)-1 5*konst2(j)+2];
    %Fast inspänd
    Kfast2(i1,i1-1:i1+2)=[0 7*konst2(j)+2  -4*konst2(j)-1 konst2(j)];
    Kfast2(in,in-2:in)=[konst2(j) -4*konst2(j)-1 7*konst2(j)+2];
    %Godtycklig inspännning
    K2(i1,i1-1:i1+2)=[0 (7-2*ins1)*konst2(j)+2  -4*konst2(j)-1 konst2(j)];
    K2(in,in-2:in)=[konst2(j) -4*konst2(j)-1 (7-2*ins2)*konst2(j)+2];
    %% BERÄKNING AV MODFORMER OCH KAPPAVÄRDEN
    Efast2=(A(i1:in,i1:in))\Kfast2(i1:in,i1:in);
    [vfast2,dfast2]=eigs(Efast2,np,'SM');
    Efri2=(A(i1:in,i1:in))\Kfri2(i1:in,i1:in);
    [vfri2,dfri2]=eigs(Efri2,np,'SM');
    E2=(A(i1:in,i1:in))\K2(i1:in,i1:in);
    [v2,d2]=eigs(E2,np,'SM');
    for i=1:np
        kappafast(j,i)=2*sqrt(dfast2(np-i+1,np-i+1))/(2*pi)/i;
        kappafri(j,i)=2*sqrt(dfri2(np-i+1,np-i+1))/(2*pi)/i;
        kappa(j,i)=2*sqrt(d2(np-i+1,np-i+1))/(2*pi)/i;
    end
end
for i=1:np
    KAPPAfast(:,i)=2*sqrt(dfast(np-i+1,np-i+1))/(2*pi)/i;
    KAPPAfri(:,i)=2*sqrt(dfri(np-i+1,np-i+1))/(2*pi)/i;
    KAPPA(:,i)=2*sqrt(d(np-i+1,np-i+1))/(2*pi)/i;
end
```

```
%%plottning av indata och resultat
%_____________________________________________________________________________
Tid=cputime-T;
disp(sprintf('%s%0.3f%s','Beräkningstid= ',Tid,' s'))
for i=1:4
    figure
    semilogx(beta,kappafast(:,i),'k'),xlabel('beta=l*sqrt(S/EI)'),...

axis([7,10000,1,1.1]),ylabel('kappa'),title(['Mode',num2str(i)]),...
        hold on
    semilogx(beta,kappafri(:,i),'r'),hold on
    semilogx(beta,kappa(:,i),'b'),hold on
    grid on
end
figure
for i=1:4

subplot(2,2,i),semilogx(beta,kappafast(:,i),'k'),axis([40,90,1,1.1]),...
        xlabel('beta'),ylabel('kappa'),title(['Mode ',num2str(i)]),hold on
    subplot(2,2,i),semilogx(beta,kappafri(:,i),'r'),hold on
    subplot(2,2,i),semilogx(beta,kappa(:,i),'b'),hold on
end
KAPPA'
%Analytiskt vid fast inspänning
%_____________________________________________________________________________
for k=1:4
    for j=1:length(beta)
        KAPPA2(j,k)=1+2/beta(j)+1/beta(j)^2*(4+(k*pi)^2/2);
    end
    figure(k),semilogx(beta,KAPPA2(:,k),'k--'),hold on
end
for k=1:4
    for j=1:length(beta)
        KAPPA3(j,k)=sqrt(1+(k*pi/beta(j))^2);
    end
    figure(k),semilogx(beta,KAPPA3(:,k),'r--'),legend('clamped',...
        'simple supported','clamped-simple','analytical clamped',...
        'analytical simple'),hold on
end
```

B.2 MATLAB Code for evaluating the value of κ and β from known End Conditions:

```
%% Hittar rätt beta värden med tillhörand kappavärden.
%_____________________________________________________________________
clc,close all
clear all
T=cputime;
%% indata
n=800;          %antal delelement
np=5;           %antal egenvärden som önskas
BETA=[70 71 72 73];                 %Gissade värden på beta
k=[1       0.991358187          0.978006327];   %Förhållande mellan
1/kappa^2 för ...
                                    %mod 2-4 som skulle ge dem samma
                                    %axialkraft
%Inspänningsgrad
ins1=0; %0=fast,1=fri
ins2=0.5;
KAPPA=zeros(length(BETA),np);      %Ska tas fram för de olika BETA-värdena
KAPPAfri=zeros(length(BETA),np);
KAPPAfast=zeros(length(BETA),np);
for i=1:n+1
    %Lastmatris
    A(i,i)=1/n^2;
end
konst=1./((BETA/n).^2);
for j=1:length(BETA)
    K=sparse(n+1,n+1);Kfast=sparse(n+1,n+1);Kfri=sparse(n+1,n+1);
    for i=3:n-1
        %Styvhetsmatris
        K(i,i-2:i+2)=[konst(j) -4*konst(j)-1 6*konst(j)+2  -4*konst(j)-1
...
                konst(j)];
        Kfast(i,i-2:i+2)=[konst(j) -4*konst(j)-1 6*konst(j)+2 ...
                -4*konst(j)-1 konst(j)];
        Kfri(i,i-2:i+2)=[konst(j) -4*konst(j)-1 6*konst(j)+2 ...
                -4*konst(j)-1 konst(j)];
    end
    %Fritt upplagd
    i1=2;
    Kfri(i1,i1-1:i1+2)=[0 5*konst(j)+2  -4*konst(j)-1 konst(j)];
    in=n;
    Kfri(in,in-2:in)=[konst(j) -4*konst(j)-1 5*konst(j)+2];
    %Fast inspänd
    Kfast(i1,i1-1:i1+2)=[0 7*konst(j)+2  -4*konst(j)-1 konst(j)];
    Kfast(in,in-2:in)=[konst(j) -4*konst(j)-1 7*konst(j)+2];
    %Godtycklig inspännning
    K(i1,i1-1:i1+2)=[0 (7-2*ins1)*konst(j)+2  -4*konst(j)-1 konst(j)];
    K(in,in-2:in)=[konst(j) -4*konst(j)-1 (7-2*ins2)*konst(j)+2];
    %% BERÄKNING AV MODFORMER OCH KAPPAVÄRDEN
    Efast=(A(i1:in,i1:in))\Kfast(i1:in,i1:in);
    [vfast,dfast]=eigs(Efast,np,'SM');
    Efri=(A(i1:in,i1:in))\Kfri(i1:in,i1:in);
    [vfri,dfri]=eigs(Efri,np,'SM');
    E=(A(i1:in,i1:in))\K(i1:in,i1:in);
    [v,d]=eigs(E,np,'SM');
    for i=1:np
        KAPPAfast(j,i)=2*sqrt(dfast(np-i+1,np-i+1))/(2*pi)/i;
        KAPPAfri(j,i)=2*sqrt(dfri(np-i+1,np-i+1))/(2*pi)/i;
        KAPPA(j,i)=2*sqrt(d(np-i+1,np-i+1))/(2*pi)/i;
```

```
    end
end
%%plottning av indata och resultat
for i=1:1
    figure,xlabel('mode number'),ylabel('constant 1/kappa^2'),hold on
    dif1=2;
    for j=1:length(BETA)
        if j==1
            plot(2:4,1./KAPPA(j,2:4).^2,'k'),title('Clamped-Free'),hold on
            plot(2:4,k(i,:)./KAPPA(j,2).^2,'k','LineWidth',1.5),hold on
        else
            plot(2:4,1./KAPPA(j,2:4).^2,'k'),hold on
            plot(2:4,k(i,:)./KAPPA(j,2).^2,'k','LineWidth',1.5),hold on
        end
        dif=k(i,:)./KAPPA(j,2).^2-1./KAPPA(j,2:4).^2;
        if abs(dif(3))<dif1
        dif1=abs(dif(3));
        a=j;
    end
    end
end
disp('Beta    Kappa 1          2          3          4         5')
disp([BETA(a),KAPPA(a,:)])
```